공학박사 학위논문

Risk-based Inherent Safety Approach to Process Design and Optimization

공정 설계 및 최적화에 대한 위험성 기반 내재적 안전성 접근법

2020년 2월

서울대학교 대학원

화학생물공학부

허 창 환

Abstract

Risk-based Inherent Safety Approach to Process Design and Optimization

Changhwan Huh
School of Chemical and Biological Engineering
The Graduate School of Seoul National University

The role of process safety is to prevent potential disasters in the chemical process. While a variety of techniques are commonly used in the field, accurate risk assessment and analysis require quantitative methods to allow direct comparisons between different alternatives or designs, among other benefits. However, there are various processes with different characteristics and complexities, and not all methods can be equally applied. It is essential to consider safety according to the characteristic of each process and to establish a design method which considers safety from the initial design stage to the operation stage. However, most process safety approaches, such as Quantitative Risk Assessment (QRA) or Hazard and Operability (HAZOP) studies, are conducted at the end of the design process and often have expansive and time-consuming drawbacks due to their repetitive nature. Therefore this thesis proposed a risk-based design method and modeling for designing an inherently safe process to consider the economic feasibility and process safety simultaneously. The thesis deals with

elements such as process knowledge management, process safety information, inherently safe design, process hazard analysis for the system configuration required to analyze, and understand the potential risk during the process design and operation. As for the process to apply this, natural gas-related processes, which are recently attracting attention due to the development of shale gas and small and medium-sized gas reservoirs were selected, to determine the optimal design of natural gas liquefaction process. In Chapter 2 of this thesis, the accident models used in the chemical process were analyzed, and the development and validation of the necessary indoor release model were addressed. Chapter 3 covered interactive simulation that uses process data during accident modeling. Finally, Chapter 4 presented a multi-objective optimization methodology to design a safer process by introducing risk modeling and inherent safety. The method is applied to the preliminary design stage of the natural gas liquefaction process and found the result that considers process safety as well as economic feasibility. The limitations of conventional designs using the concept of inherent safety were overcome by implementing the quantitative risk assessment procedure directly in the optimization sequence.

Keywords: Risk-based Design, Risk estimation, Inherent Safety, Quantitative Risk Assessment

Student Number: 2014-21537

Contents

List of Figures

List of Tables

Chapter 1. Introduction

1.1. Research motivation

The world of the chemical process is diverse, and every process has different characteristics depending on its chemicals, construction materials, and scale. However, process safety management is always conducted in the same way to assess the risk of the process occurred from outcomes of accidents. Hazard identification and process safety techniques are used during the various stages of the process life cycle (Figure 1.1), and safety assessments are required to assess and analyze the degree of process risk and hazard to ensure process safety.

However, safety assessments do not always guarantee the safety of the process. As shown in Figure 1.2., among 68 cases of chemical accidents investigated by U.S. Chemical Safety and Hazard Investigation Board (CSB), 22 cases had occurred even though mandatory process hazard analysis (PHA) was conducted beforehand.[1] Therefore, it is essential to establish methods for chemical process design considering safety both starting from an early design stage to operation and design modification stage. More early the safety is considered, the risk reduction effectiveness increases.

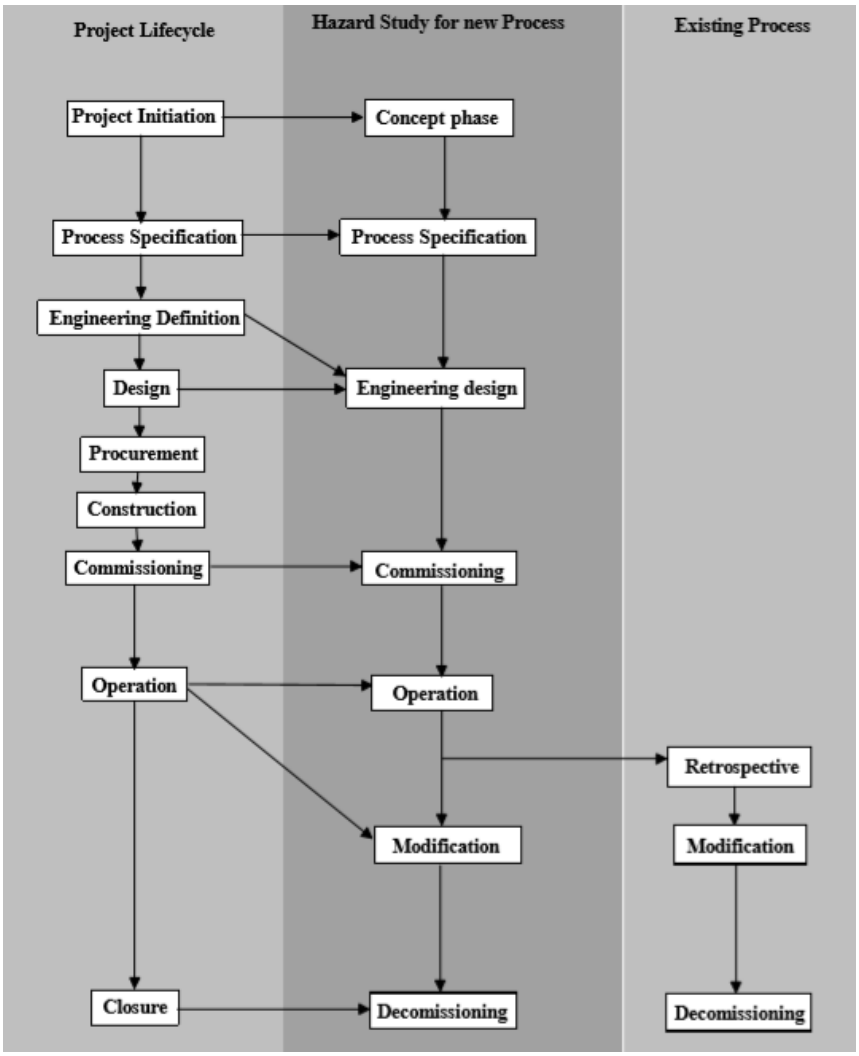

Figure 1.1 Hazard identification in the process life cycle [2]

Table 1.1 Main and contributing causes of accidents as derived from CSB reports [1]

	Number of cases	Percentage
No adequate safeguards	38	55.9%
Operation and maintenance issues	30	44.1%
Abnormal and non-routine operations	38	55.9%
Human & Organizational factor issues	39	57.4%
Process Hazard Analysis issues	22	32.3%
Facility siting close to public or personnel issues	32	47.1%
Non-compliance with industry standards	26	38.2%

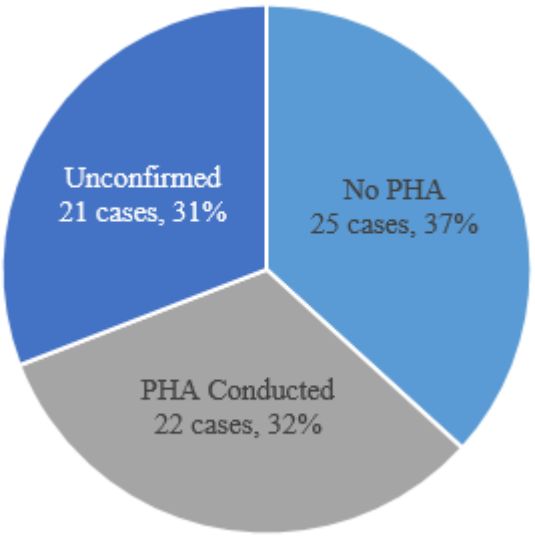

Figure 1.2 Chemical accident cases regarding PHA derived from CSB reports [1]

1.2. Research objective

The problem this thesis tries to solve is how to manage the risk fundamentally during the general procedures of process design. The process design starts from the conceptual design stage, where unit operations and optimization studies are performed, and making process flow diagrams (PFD) and heat and material balances (H&MB) sheets. The thesis will discuss the advanced process design strategy approach in an attempt to develop a new method of decision making in the context of process safety and process systems engineering.

Particularly, among various processes in the overall natural gas supply chain, this thesis dealt with liquefaction and end-user distribution. For designing a safer natural gas processing, a new method of deciding an optimal design of the LNG liquefaction process through multi-objective optimization for minimizing the total annual cost and the potential risk was proposed. The natural gas sources become unconventional, varying from small size reservoirs and shale gases recently. This change makes sustainable production of LNG with leaner feed natural gases with strict safety requirements necessary. Therefore, the application of the method to the oil and gas industry is significant.

For addressing these objectives, several process systems and safety technologies, including interactive simulation, multi-objective optimization, and inherent safety, are developed and implemented. Understanding hazards and risks cover the systems and information required to analyze and understand the type of potential hazards during the process design and operation. It includes the following elements which will be covered in this thesis; Process knowledge management, process safety information, inherently safer design, process hazard analysis, risk analysis, and capital project review.

1.3. Outline

The remainder of the thesis is organized as follows. Chapter 2 discusses the consequence modeling in process safety. The Chapter also presented a new simplified indoor release model and its validation. Mitigation analysis was conducted based on the model. In Chapter 3, a process-accident interactive simulation was studied using consequence models presented in Chapter 2. Case study of city gas pressure regulation station was performed, and the results were compared with conventional QRA software to verify the validity of the interconnection between the process simulation and the accident simulation and usage of dynamic process data into the consequence analysis. In Chapter 4, the new methodology was proposed and applied for designing optimal operating conditions of three different natural gas liquefaction processes considering the inherent safety and economic feasibility. Lastly, in Chapter 5, the conclusion of the thesis is presented.

The works presented in Chapter 2 and Chapter 4has been submitted to *Journal of Loss Prevention in the Process Industries* and *Industrial & Engineering Chemistry Research*, respectively.

Chapter 2. Accident models in Chemical Process Industries

2.1. Introduction

The most dangerous chemical process accidents that cause a massive amount of life and property damage involve leakage of toxic or flammable chemicals. The primary damage caused by the leak is based on the atmospheric dispersion of the chemical, in addition to the fire and explosion accidents, where the confined hazardous chemical ignites. It is necessary to determine the amount of chemicals and their concentration accurately within a short period to organize a proper accident response to minimize the damage. However, when there is a need to assess such post-event effects, most damages are already inflicted before the accurate measurement since it requires several preparations and takes a relatively long time compared to the consequence modeling. Therefore, to organize a suitable response in a time of need, and to assess the safety of a location, dispersion of gas and its concentration profiles are required to be estimated through the quick, and yet accurate modeling.

While the input variables of dispersion calculation vary with models, typical models include discharge pressure, discharge temperature, overall discharge time, and flowrate. Additionally, it further requires wind direction and other weather conditions to calculate the effect zones.[3] The climate information can be acquired from external sources, but discharge information should be acquired either through measurement or calculation. However, the sudden nature of the chemical accidents prevents accurate, timely measurement of the discharge rate and other information during incidents. Thus, like the overall

consequence modeling mentioned before, engineers have often relied on modeling and calculation when obtaining the discharge rate as well.

In this chapter, effects and the importance of consequence modeling in the process safety were briefly discussed. Then the development of the indoor release model, which calculates gas flowrate and concentration during an indoor gas leak is presented. If an accidental gas leak occurs inside a building, the effect of the building must be predicted. While Computational Fluid Dynamics (CFD) is a useful method that provides accurate prediction, it is only possible under sufficient resources to obtain accurate results. Without sufficient time to simulate, specific information to calculate, and human effort to organize, application of CFD in the field of process safety is limited. The indoor release model modifies the release flowrate and concentration of discharge flow for the dispersion calculation in much simpler terms. Validation and verification of the model for average indoor gas concentration are done, demonstrating its accuracy. While the model may not predict complex mixing to the level of CFD, it provides compatible predictions with far less time and modeling parameters. The additional studies carried out show that under several occasions, the building can work as an effective mitigation method against hazardous gas leaks by diluting the concentration of gas released and restricts the dispersion area, implying the necessity of the developed model.

2.2. Analysis of conventional accident models for chemical processes

A wide variety of research has been done on discharge source models and dispersion models, including comprehensive studies on accidents [4], specific discharge models, dispersion models for generalization[5], and the subsequent consequences.[6, 7] Discharge and subsequent models are vital in consequence modeling, QRA, and other safety studies since conventional risk assessment methods and software are conducting their assessment based on these models. However, model mismatches can occur during the process. For one, many accident simulations assume steady or static input. This limits of dynamic input in accident simulation, which may be available from process data. For instance, a short pipe discharge model in Phast and SAFETI assumes the pipe that the leak occurs is connected to the static reservoir, therefore requires static inventory. However, if there is no reservoir or storage and no alternative is given, the engineer is presented with little choice.

For an operating system, static inventory modeling needed to be obtained from process flow data. The equation for estimating static inventory in the continuous system, I, is presented below.

$$I = \rho_f \times D \times L + \frac{M}{t_{isolation}} \tag{2.1}$$

ρ_f is fluid density (kg/m^3), D and L is inner diameter (m), and length (m) of the target pipeline and vessel, respectively. M is initial mass stored (kg), and $t_{isolation}$ is isolation time (s), the time required to isolate the source.

In the case of discharge modeling, things become more complex.[8, 9]

$$Q = \rho A C_D \sqrt{2[\frac{g_c P_g}{\rho} + g_c h_L]} \tag{2.2}$$

$$Q = C_D A u_o \div v_o \tag{2.3}$$

$$Q = C_D A \sqrt{\frac{c_p}{c_v} \rho_0 P \left(\frac{2}{\frac{c_p}{c_v}+1}\right)^{\frac{\frac{c_p}{c_v}+1}{\frac{c_p}{c_v}-1}}} \tag{2.4}$$

$$Q = YA \sqrt{\frac{2 g_c \rho_1 (P_1 - P_2)}{\sum K_f}} \tag{2.5}$$

There are several equations that describe fluid discharge models. Equation (2.2) describes the behavior of liquid discharge based on the Bernoulli equation, while (2.3) is the fundamental equation of discharge with isentropic expansion, (2.4) is for choked gas flow, and (2.5) is for ideal gas flow, where, Q = discharge mass flowrate (kg/s); A = discharge area (m^2); C_D = discharge coefficient; g_c = gravitational constant(m^3/s^2kg); $u_o =$ velocity(m/s); v_o = volumetric flowrate of discharge(m^3/s); P = pressure(Pa); $\frac{c_p}{c_v}$ = heat capacity ratio; Y = gas expansion factor; K_f = excess head loss.

Appropriate usage of suitable model is mandatory for precise accident modeling and risk estimation, since the results from the discharge source models are directly applied as an input to the other models; (e.g., dispersion, pool generation, fire, and explosion) The successive consequence models should be changed, based on the types of the output from the previous model which works as an input, and the circumstances and the assumptions made in them. For instance, if a pool fire model uses a steady form of input, assuming a static liquid pool while the pool was generated based on the liquid leak, which is dynamically changed, the result would be far from ideal.

The further consequences in the thesis are calculated through corresponding consequence models. These models are further explained in section 4.2.

2.3. Development of indoor release model

While studying consequence models mentioned in the previous section, it was found out that there was a lack of verified models in regard to indoor gas leaks. As the results from the discharge source models are directly applied as an input in the dispersion calculation, it is assumed that the discharge takes place on the outside, and the gas begins to be dispersed to the atmosphere simultaneously. However, direct application of discharge model results for the dispersion calculation is valid only if all materials are immediately released to the atmosphere. If the leak occurs in a building or a confined space (e.g., indoor plants, storage facilities, or pipelines), immediate dispersion calculation should be invalid because the leaked gas is mixed with the air inside the building first and then released to the atmosphere. Hence, a model for the gas leaked from the interior of the building requires an additional, different approach to the discharge source model before the calculation of atmospheric dispersion.

Most researches regarding the indoor gas leak focus on the indoor dispersion behavior of the gas. These researches aim to analyze explosion limits of the gas since the leak in the confined space can be deployed into fire and explosion. Woodward et al. used a numerical mass balance to simulate a flammable concentration of gas evaporated from a liquid pool.[10] An application of computational CFD is also becoming popular lately. Wu et al. applied CFD to the indoor leakage of flammable, explosive gas to analyze the indoor gas concentrations.[11]

On the other hand, Montoya et al. surveyed models for mapping the indoor toxic gas concentration as a function of the outdoor concentration.[12] The purpose of such models is to estimate the effectiveness of taking shelter when

an accidental release of toxic gas occurs at the outside of the building as the indoor concentration would be lower than the outside concentration. On the contrary, when the release occurs inside, the toxic gas release to the outdoors should be limited because of the building. This limitation decreases the amount of gas released to the outdoors, in the form of decreased concentration and flowrate.

While several studies have been done regarding the indoor gas dispersion and distribution, there exist only a couple of models regarding the effect of the indoor release on the outdoor dispersion. Moreover, they focus on the distribution of gas in the interior rather than release to the exterior. For example, Phast, one of the most widely used software for the process hazard analysis, has an in-building gas leak model called INBU. Functions of the INBU model include calculating indoor concentration from a leak inside a building and modifying the source terms before solving a dispersion model. The result of the aforementioned in-building release calculation is applied to the outdoor dispersion model with the modified droplet size, new discharge velocity, and discharge direction. The release rate of the INBU model is based on simple mass balances. In addition, the INBU model does not provide validations nor verifications.

Deaves et al.[13] and Gilham et al.[14] presented a model that calculates the rate of release of dense vapor from a building. It is one of the few validated models that can be applied to atmospheric dispersion. The mixing models presented in these studies are concerned with gas released into a building, for both isothermal and non-isothermal cases. The main limitation of the Deaves' model is its complexity associated with its incorporation with CFD. While CFD offers high accuracy, the computational requirement is prohibitive for practical

applications, particularly for using the model in taking emergency actions. Although the computation time depends on various circumstances such as grid size and governing equations, CFD is unsuitable for damage prediction and organizing responses since it requires the time not only for computation but also for creating relevant CFD geometry.

The objective of this section is to suggest a suitable model that calculates outdoor flowrates and concentrations in case of an indoor leak. Accuracy is an important issue since most existing models remain to be validated.[10, 11, 15] The model is validated with existing experimental data and further verified by comparing it with CFD simulation results. Meanwhile, the model should be simple and concise enough to be calculated fast, as well. Moreover, it should also accept various types of discharges as inputs. The model is also required to calculate material flowrate to the outdoor atmosphere and average indoor concentration of the chemical when it is released from the interior of the building. Lastly, the model should be robust enough to be applied and used for most of the indoor release incidents. The applicability of the model decreases when the model becomes more complex.

Indoor release model description

Inflows and outflows through vents should be balanced against each other. This gives,

$$v_{out} = v_{in} \tag{2.6}$$

While the outflows are limited to vent emissions only, the inflows are the entire flow of gas generated inside the room, include both generated gas flow from the leak and airflow from the exterior. The gas that forms generated gas flow can be either the gas released directly from the source or the gas evaporated from the liquid pools formed by the leak.

If there is only a single vent, the vent is fully occupied with the emission. The airflow from the exterior to the interior would not exist in this case. However, the multiple vents separately positioned enable the air movement throughout the room and provide additional ventilation flow. External flow from the outside and the same amount of the volumetric flow is added to maintain the overall volumetric balance.

$$v_{out} = v_{in} = v_o \tag{2.7}$$

$$v_{out} = v_{in} = v_o + v_w \tag{2.8}$$

While volumetric flowrates from and towards the building are equal, the concentration profiles of each flow are different. The released gas is diluted with the indoor air before being released to the atmosphere. Deaves et al.[13] derived the concentration profile of the released material from the material balance of the room and expressed as 2.9, which is a function of time and volumetric flowrate, then further derived 2.10.

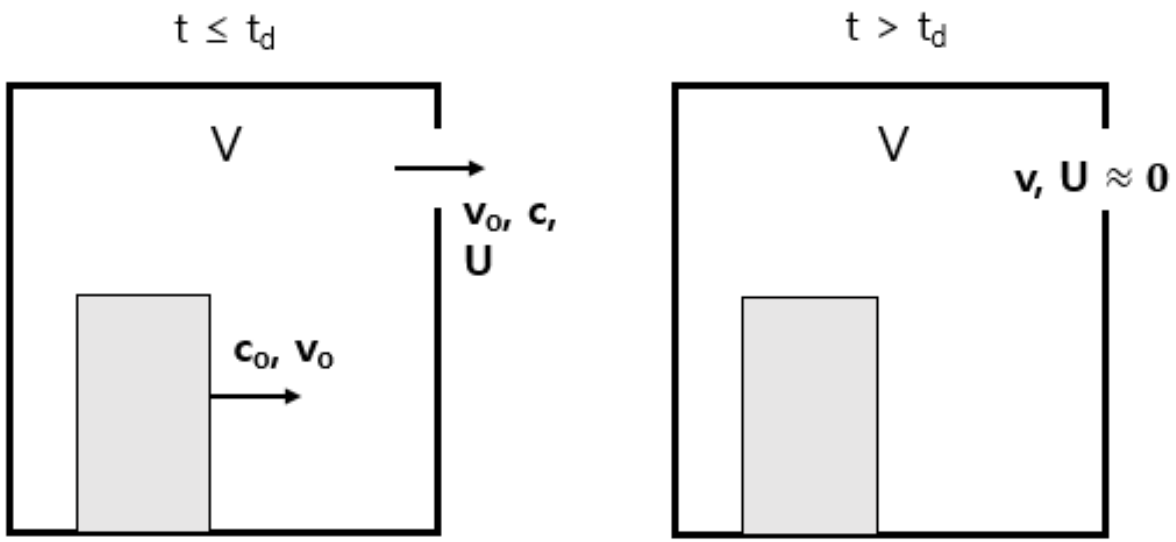

Figure 2.1 Diagram of model releasing from a building with a single vent

$$\frac{dc}{dt} = \frac{(c_o - c)v_o}{V} \tag{2.9}$$

When there is no more release (v_o = 0), the release to outdoor also stops.

$$\mathrm{c} = c_o(1 - e^{-\frac{v_o t}{V}}) = c_o(1 - e^{-\frac{t}{t_v}}) \quad (\mathrm{t} \le t_d) \tag{2.10}$$

$$\mathrm{c} = c_o(1 - e^{-\frac{t_d}{t_v}}) \quad (\mathrm{t} > t_d) \tag{2.11}$$

The equations of the indoor release with multiple vents are different from the release with a single vent. The worst-case scenario when the emission is the largest is when the vents are located on the opposite sides.[16] Therefore, we derived the following equations assuming the worst-case scenario.

$$\frac{dc}{dt} = \frac{(c_o - c)v_o - cv_w}{V} \tag{2.12}$$

$$\mathrm{c} = \frac{v_o c_o}{v_o + v_w}\left(1 - e^{-\frac{(v_o + v_w)t}{V}}\right) = \frac{v_o c_o}{v_{out}}\left(1 - e^{-\frac{t}{t_{vw}}}\right) \quad (\mathrm{t} \le t_d) \tag{2.13}$$

$$\mathrm{c} = \frac{v_o c_o}{v_{out}}\left(1 - e^{-\frac{t_d}{t_{vw}}}\right)e^{\frac{t_d - t}{t_w}} \quad (\mathrm{t} > t_d) \tag{2.14}$$

The corresponding volumetric flow is,

$$v_{out} = v_o + v_w \quad (\mathrm{t} \le t_d) \tag{2.15}$$

$$v_{out} = v_w \quad (\mathrm{t} > t_d) \tag{2.16}$$

If there is no ventilation but forced ventilation in the room, the volumetric flowrate to the outside is fixed to the flowrate of forced ventilation.

$$c = c_o(1 - e^{-\frac{v_f t}{V}}) = c_o(1 - e^{-\frac{t}{t_{vf}}}) \tag{2.17}$$

For a time-varying, dynamic discharge, the same volumetric balance is applied. For a validation purpose, the discharge flowrate was estimated as a function of time, applying the finite difference method. The corresponding volumetric flowrate and concentration are,

$$v_{out} = v_o(t) = v_{o,i+1} + \frac{(v_{o,i} - v_{o,i+1})(t_{i+1} - t)}{t_{i+1} - t_i} \qquad (t_i \le t < t_{i+1}) \tag{2.18}$$

$$c = c_o - (c_o - c_i)e^{-\frac{(t-t_i)(\frac{v_{o,i+1}-v_{o,i}}{2} + v_{o,i}t_{i+1} - v_{o,i+1}t_i)}{V(t_{i+1}-t_i)}} \qquad (t \le t_d) \tag{2.19}$$

$$c = c_o - (c_o - c_{d-1})e^{-\frac{v_{o,d-1}(t_d - \frac{1}{2})}{V}} \qquad (t > t_d) \tag{2.20}$$

c_i indicates the concentration of the released chemical at discrete time point t_i. Each concentration at the designated time can be obtained from the concentration at the previous time step. After the end of the discharge, $v_{o,i+1}$ equals zero, and the interior concentration becomes stagnant. If there are multiple vents, the flow characteristics can be estimated as follows,

$$v_{out} = v_o(t) + v_w = \frac{v_{i+1} + v_i + 2v_w}{2} \tag{2.21}$$

$$c = c_i e^{\frac{-v_{out}(t-t_i)}{V}} + \frac{v_{i+1} + v_i}{v_{i+1} + v_i + 2v_w}(1 - e^{\frac{-v_{out}(t-t_i)}{V}}) \qquad (t \le t_d) \tag{2.22}$$

$$c = \left(c_{d-1}e^{\frac{-v_{out}(t_d-t_i)}{V}} + \frac{v_{d-1}}{v_{d-1}+2v_w}\left(1-e^{\frac{-v_{out}(t_d-t_i)}{V}}\right)\right)e^{\frac{t_d-t}{t_w}} \quad (t > t_d) \tag{2.23}$$

In this case, the interior concentration continues to decrease since there is more active material exchange compared to the case of the single vent.

Several assumptions have been made to make the calculation feasible. It is assumed that the material exchange between spaces exists only between the outdoor atmosphere and the room where the leak occurs. That is, there is no material exchange between different rooms, and the building interior is considered a single zone. The amount and partial pressure of the released material are assumed to be not high enough to cause choked flows at vents or harm the structures of the building. The occurrence of choked flows means the room is significantly over-pressured, which may cause destruction or strain of the physical structure of the building. Calculating strain of the building requires another independent research and is not considered here.

Mixing ventilation was assumed to be the type of ventilation taking place in the building. During mixed ventilation, the concentration and the resulting temperature were assumed to be uniform in the zone, under a developed, properly designed mixing ventilation system.[17, 18] The ventilation type depends on the vents to the outdoors and the existence of forced ventilation. Since the model illustrates the release of the indoor chemical from the interior to the exterior, there should be one or more vents in the room.

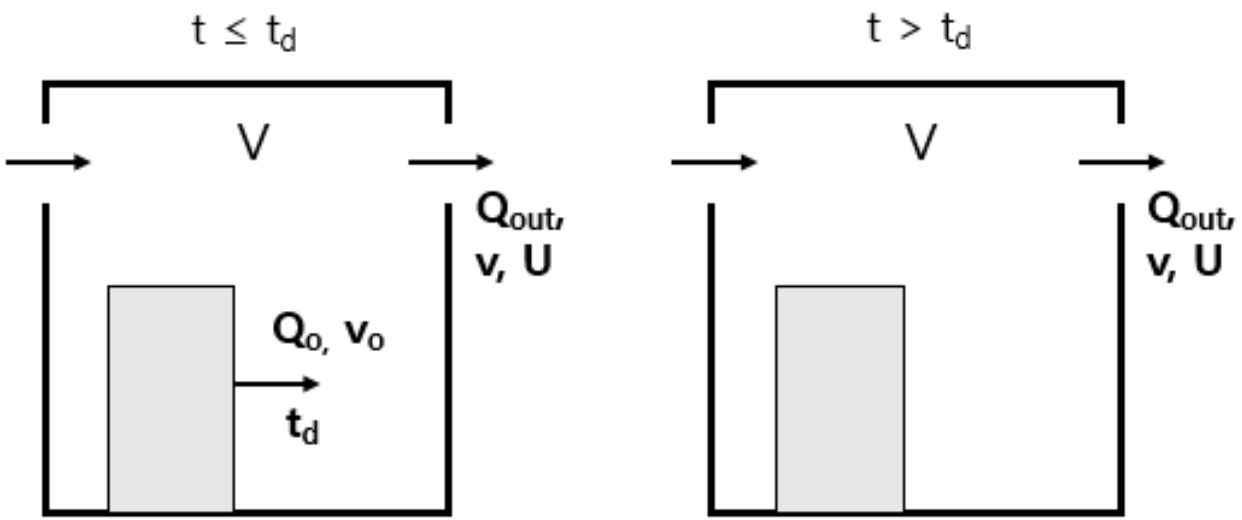

Figure 2.2 Diagram of model of releasing from a building with multiple vents

The concentration and the pressure at the vent exit are assumed to be average concentration and pressure of the room. A CFD or similar rigorous model is required to calculate the concentration accurately, which is not suitable to calculate release flowrate in a short time. We also neglect the dispersions through the vents driven by the concentration gradients. Lastly, the vent size is small enough for the room to be distinguished from the exterior.

As with the dispersion velocity and concentration, the indoor release rate is a function of wind speed. Even though the interior is separated from the exterior by walls, the indoor air movement still exists regardless of the existence of external wind. Wind inside a building can be caused by various reasons such as forced ventilation between interior and exterior or natural air convection. A survey of wind speeds in indoor workplaces has been done by Baldwin and Maynard.[19] The measurement yielded an arithmetic mean of 0.3m/s. It was also noted in the survey that there is no discovered correlation between wind speed distribution and physical conditions such as room size or ventilation type. Unless they are measured, the observer cannot quantitatively obtain or calculate indoor air movement and speed while chemical discharge occurs. Therefore, we used 0.3m/s as a default internal wind ventilation speed.

Every discharge can be classified into gas discharge, liquid discharge, or two-phase discharge by the phase it is released. In the case of the indoor discharge of the liquid, most of the discharged material is trapped inside as the form of liquid pools. However, when the discharge includes a gas phase, the material can be exchanged freely through vents. The key point of the model is describing inhibition caused by the building to differentiate between free atmospheric release

and the indoor release. The discharge can also be classified as instantaneous or continuous by discharging duration. Then continuous discharge models can be classified further as a constant or time-varying model accordingly, whether the discharge rate changes or not during the calculation. The indoor release model should be able to accept these various types of discharge model outputs as input variables.

Model validation and verification

Gilham et al.[20] conducted several experiments on gas build-up within a single building volume at Silsoe Research Institute. Results of the six runs were provided with time-course experimental data of gas concentration. Carbon dioxide was released in a 2.44m^3 cube, at two different constant flowrates (600L/min and 950L/min). The release duration is 5 minutes (Run 3, 4, 5) and 3 minutes. (Run 6, 7, 8) While the experiments had not measured any flowrates, they had measured the interior concentration of CO_2 at several different points within the cube to measure the internal gas dispersion behavior. To verify the indoor release model, the average concentration of carbon dioxide in the cube was calculated by dividing the sum of the concentrations at each point, multiplied by their relative height differences with an overall height of 2.44 m.

It was noted in the experiment that the concentration of the inlet gas flow is not pure. The gas supply was diluted by the air since there was an inflow of air into the CO_2 storage. The diluted molar concentration of the CO_2 source is 70 to 80%. The CO_2 concentration of the inlet flow used in validation was set to the same value from the release conditions of the runs for indoor release model calculation. Some data from Run 3 was out of range and had to be estimated.

The comparison results are presented in Figures 2.4 and 2.5 and Table 2.1. The model estimates the general tendency of interior gas-build ups. Comparing Figures 4 and 7 to the rest shows that the indoor gas concentration decreases after the release duration in multiple-vent scenarios. This indicates the gas still emits from the building even after termination of the initial discharge, which will further affect the dispersion. However, in single-vent scenarios, the indoor gas

concentration remains relatively stagnant. This makes the previous assumption of neglecting the diffusion caused by the concentration gradient feasible. It is concluded that the model reasonably describes the gas flowrate to the outside of the room where the chemical leak occurs at constant discharge flowrate over time with some reservations.

Figure 2 shows the indoor concentration decreases over time more rapidly than the estimation model predictions. The decrement of the concentration is dependent on the indoor wind speed. Since the experiment did not measure the wind speed of the indoor site, the model used the average indoor workplace wind speed value of 0.3m/s.[19] The mismatched wind speed would have caused a difference in the concentration decrement.

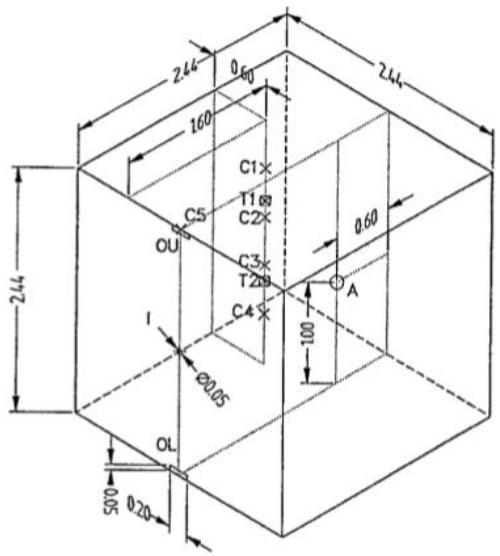

Figure 2.3 Schematic diagram of the test room in centimeters [20]

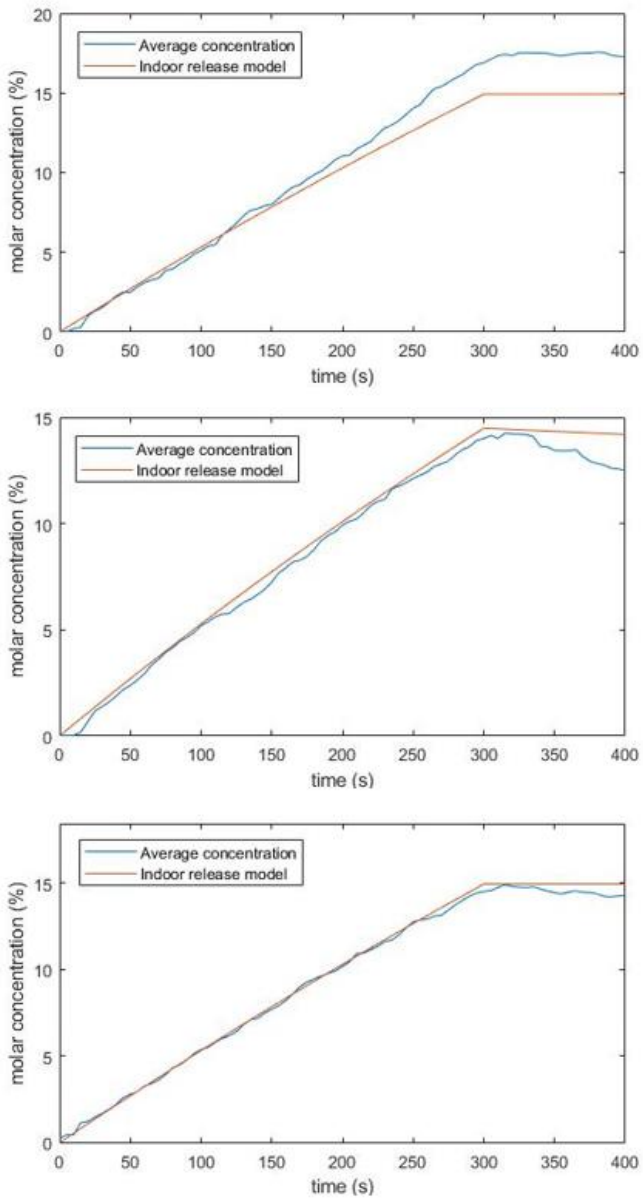

Figure 2.4 Comparison of modeling result with measurement for Run 3 (Top, Upper vent open, 600L/min), 4 (Middle, Both vents open, 600L/min), 5 (Bottom, Lower vent open, 600L/min)

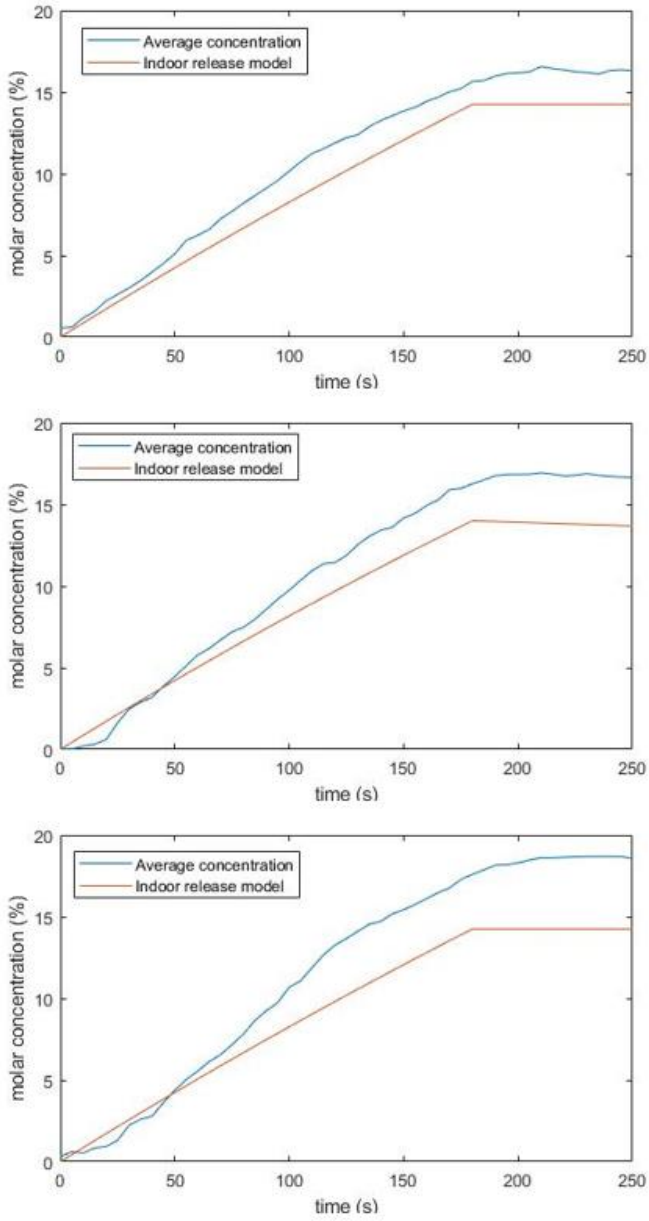

Figure 2.5 Comparison of modeling result with measurement for Run 6 (Top, Lower vent open, 950L/min), 7 (Middle, Both vents open, 950L/min), 8 (Bottom, Upper vent open, 950L/min)

Table 2.1 Comparison of carbon dioxide concentrations at t_d

Run number	Carbon dioxide concentration at t_d (%)	
	Experiment	Model
3	16.89	13.06
4	14.01	12.68
5	14.50	13.99
6	15.66	14.25
7	16.26	14.00
8	17.59	14.25

To further assess the applicability of the model, it was compared to more accurate CFD simulations. FLACS of GexCon was used to verify the model and evaluate the impact of the release. FLACS is a three-dimensional CFD software that can analyze fire and dispersion caused by chemical accidents. FLACS calculates the solution of vapor cloud dispersion for a compressible fluid by the Reynolds Averaged Navier-Stokes equations using a finite volume method. For a turbulent closure, it is coupled with the k-ε model with the standard set of constraints.[21] The boundary layer for the atmosphere is set by the velocity. The simulation results were compared to the corresponding experimental data of Run 6 to verify the reliability of FLACS. The comparison result of the average carbon dioxide concentration is shown in Figure 9, by measuring CO_2 concentration at the same points in the experiment. The total volume of the space for the simulation was set to be $12.5 \times 12.5 \times 5.1 m^3$, which includes the building itself and the surrounding areas. The total number of grids used in the simulation was 305,140. There is little difference in the average interior concentration of carbon dioxide between the experiment and the simulation results.

More simulations were conducted after verifying the reliability of the FLACS simulation. Leak and vent conditions were changed to verify the relation presented in the indoor release model. A horizontal leak of carbon monoxide is considered in a building whose size is $10 \times 10 \times 5 m^3$, with the two ventilation areas having the same size of $2.5 m^2$. The most notable difference between the two calculations was computational time. While the indoor release model took mere seconds, FLACS took a minimum of an hour and more, depending on the geometry.

The concentration calculated from the indoor release model is generally lower than the measurements from the experiment or CFD simulation. Higher concentration development than the model means more gas is accumulated within the building than anticipated. The simulation results of the 950L/min release rate are similar to the concentration accumulation when the source is not diluted with air. When comparing the concentration profiles of the experiment runs that have the same inlet flowrate but different vent positions (Run 3 with Run 5 and Run 6 with Run 8), one can notice that the concentration from the experiments where only the upper vent was opened, Runs 3 and 8, are higher than their counterparts, Runs 5 and 6. The main reason for these differences is that carbon dioxide is heavier than the air and possesses a tendency to flow down. Concentrations of upper vent cases are higher than the lower vent cases, indicating dense gas will accumulate in the lower level of the building. General lower estimation, which means higher gas concentration for the outdoor flow, can be explained similarly. First is inconsistency in the mixing, where released gas is not uniformly distributed. Second is the gas behavior becomes less incompressible if the relative flowrate over the volume of the building is increased.

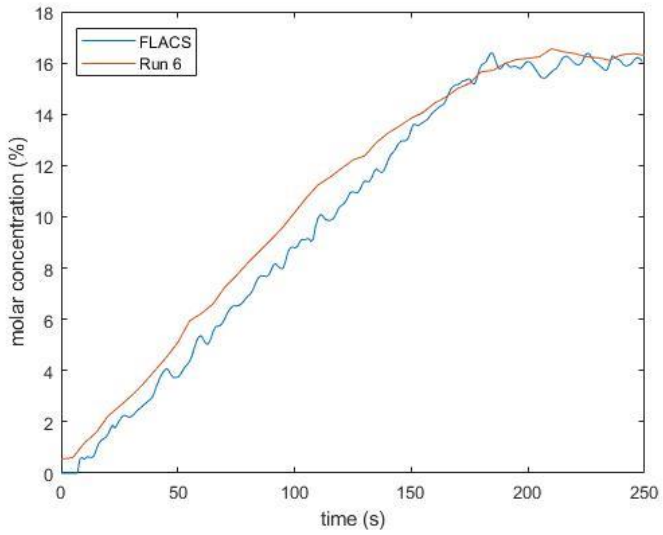

Figure 2.6 Comparison of simulation results with measurement for Run 6

Table 2.2 FLACS simulation condition and data

Simulation Number	1	2
Release material	Carbon monoxide	
Interior Volume(m^3)	500	
Release duration(s)	100	
Discharge rate(kg/s)	10	5
Discharge rate(m^3/s)	5.775	2.880

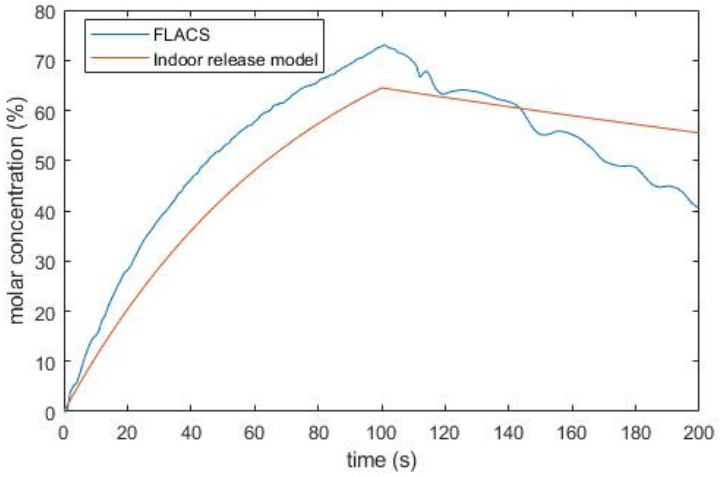

Figure 2.7 Comparison of modeling result with simulation 1

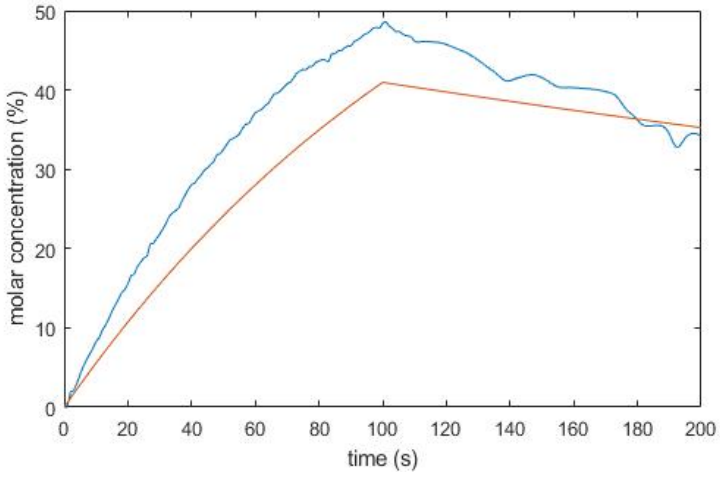

Figure 2.8 Comparison of modeling result with simulation 2

There are time delays when comparing the experimental data with the indoor release model results. Both the time when the concentration of the rapid indoor gas starts to increase and the time when the maximum concentration of the indoor gas is reached are several seconds later than the time the model had anticipated. Time delays vary from 5s to 30s for each run. This is most likely due to the required time for the released gas to finally reach the sensor and the vent, respectively.

The concentration and time difference between the experiment and the model indicate that due to the interior volume of the building, the leaked gas requires time to disperse and reaches the ventilation point. If the air is not well-mixed, less concentrated gas may release from the building initially, resulting in higher concentration. Using CFD simulations can prevent this discrepancy; however, it requires accurate indoor geometric information. While the indoor release model cannot predict the occurrence and the effect of the time delay, it is still possible to apply the results to atmospheric dispersion since the dispersion model is affected by the release duration, not the time when the release begins. Time delay and lowered release concentration imply that the building can be used as a mitigation method.

2.4. Mitigation effect analysis

Mitigation effect study was conducted to stress out the significance of the developed model. The building that contains the leak affects the release concentration and flowrate to the atmosphere and can be used for mitigation purposes. In practice, the material exchange through the vent still occurs either through the form of gravity-driven counterflow or diffusion.[22] However, as shown in the validation, this effect is almost negligible. Hence, in order to show how the indoor release qualitatively affects dispersion, atmospheric dispersion of the gas released from the building over time was simulated, assuming the wind is the only driving force. Once again, CFD simulation was used, in this case, to obtain more precise results. CO dispersion under both of the indoor and outdoor release conditions at Ulsan industrial site, Korea, was examined with Flacs simulation results. It can be concluded from the simulation results that the dispersion behavior from the leak differs by the existence of the building that the leaks occurred. Alteration of the release duration and concentration caused by indoor release not only reduced the concentration of the dispersed gas but also made the gas remain longer in the area when the wind is not fast enough to disperse the gas.

To quantitatively evaluate the mitigation effect of the building, a different set of simulations was conducted defining mitigation effectiveness at each specific location. The same variable was defined in previous research by Lim et al. to study effective mitigation systems with different sizes of barriers.[23]

Mitigation Effectiveness at a given point is defined as,

$$\text{Mitigation Effectiveness (\%)} = \frac{C_{No,max} - C_{A,max}}{C_{No,max}} \times 100 \quad (2.24)$$

where $C_{No,\ max}$ is maximum concentration with no building and $C_{A,\ max}$ is Maximum concentration with a building with vent area of A.

The simulations were conducted as they change conditions each time to find a relationship between ventilation area and atmospheric gas dispersion. For the discharge duration of 100s, two different discharge rates, 5kg/s and 10kg/s, and six different ventilation areas, 0.4, 0.6, 0.8, 1.0, 1.5, and 2.0 m^2 were considered. The ventilation area was controlled by modifying the height of the vent while its length was fixed at 1m.

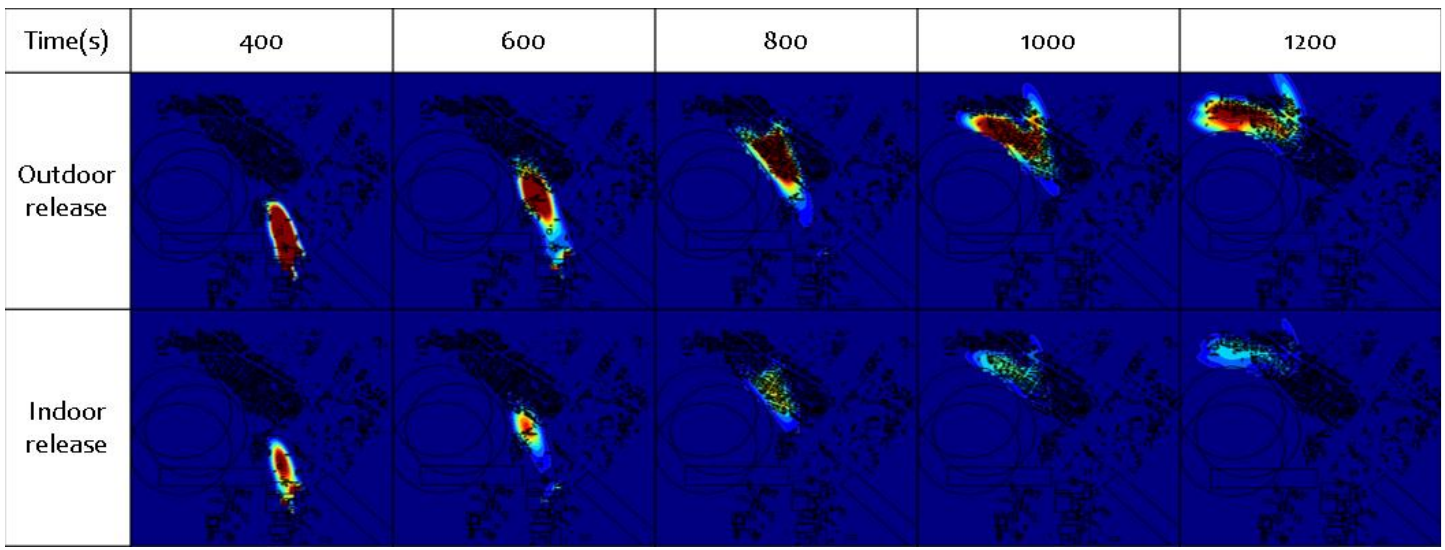

Figure 2.9 Comparison of CO dispersion between outdoor release and indoor release (with single vent)

(Blue: 0% CO, Red: over 0.01%)

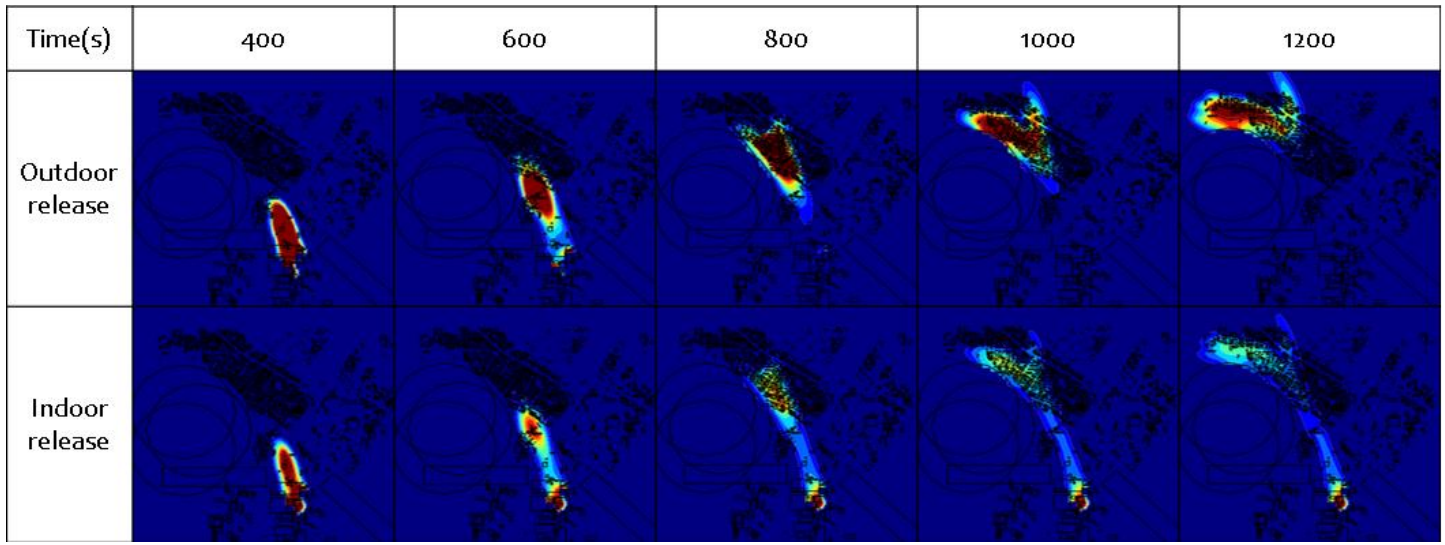

Figure 2.10 Comparison of CO dispersion between outdoor release and indoor release (with multiple vents)

(Blue: 0% CO, Red: over 0.01%)

The results showed that small vents concentrate released gas to a narrow line, causing even higher concentration than standard outdoor leaks. While a significant portion of the leaked gas remains in the building and the overall dispersed area is smaller, the maximum gas concentration in the case of the 0.4 m^2 vent was higher than when no building was presented, causing negative mitigation effectiveness. Negative mitigation effectiveness implies that the building does not work as mitigation. This indicates that small vents force leaked gas to focus on a specific direction. Instead of being dispersed widely with a relatively low concentration, the gas spreads narrowly with a higher concentration. While the exact required area is related to the gas discharge rate that fills the building, it can be concluded that a small vent may cause even more damage despite the low discharge rate.

On the other hand, a sufficiently large vent can mitigate gas dispersion effectively. Among the results, the building mitigates the leak when the vent area is over 0.8 m^2. However, it should also be noted that mitigation effectiveness decreases as the vent area exceeds a certain threshold. Needlessly large vent decreases the mitigation effect. As the vent area increases, the building condition becomes similar to the atmospheric condition and the behavior of the release to the outdoor approaches that of the direct release to the atmosphere.

Lastly, the effect of the mitigation of a building is more apparent when the distance is longer. Both the time gap and the mitigation effectiveness increase as the distance of the target location from the building increases. While long-range dispersion is profoundly affected by the wind speed and direction, even a minor mitigation measure proves effective when its effect is accumulated. This means the building can affect much larger when calculating the risk at a remote location.

Table 2.3 Comparison of mitigation effectiveness to vent area and discharge rate

Distance (m)	Discharge rate (kg/s)	Vent area (m2)					
		0.4	0.6	0.8	1	1.5	2
100	5	-10.7	-41.4	29.6	27.8	61.7	41.0
	10	-71.6	46.5	12.8	34.5	25.9	19.1
200	5	25.7	-16.1	40.1	45.7	57.4	47.6
	10	-21.8	43.2	49.7	56.5	40.0	26.6

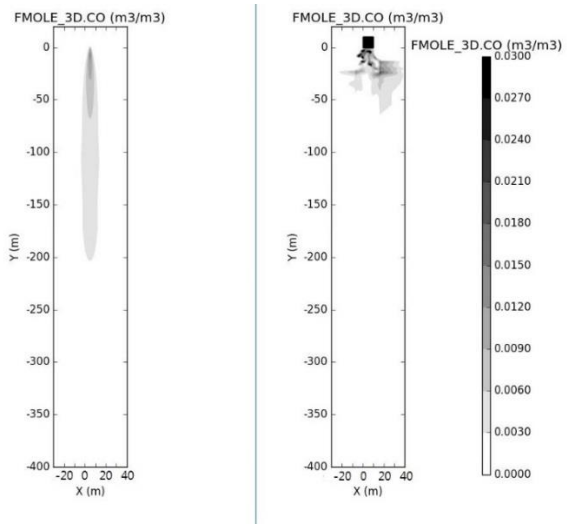

Figure 2.11 2D contour of CO at 50 s (Left: Outdoor, Right: A building with $2m^2$ vent).

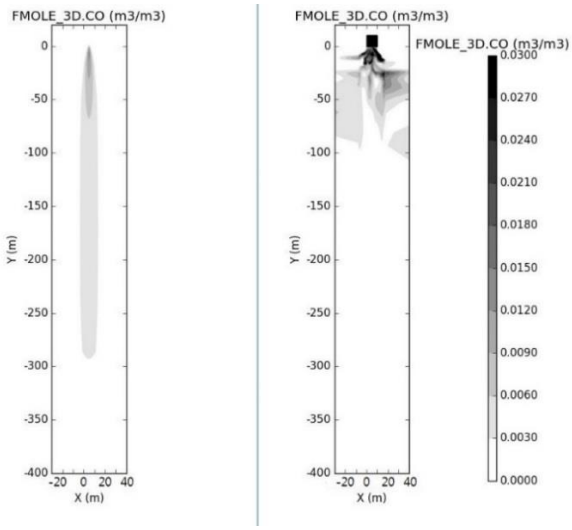

Figure 2.12 2D contour of CO at 100 s (Left: Outdoor, Right: A building with $2m^2$ vent)

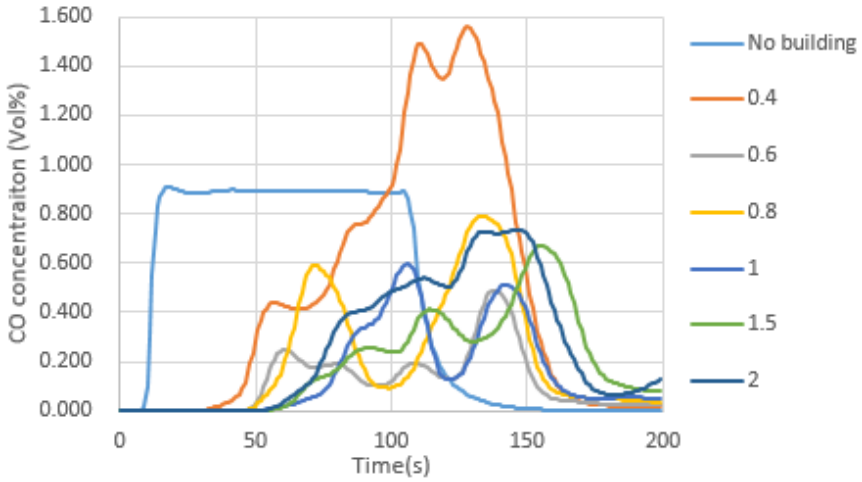

Figure 2.13 Concentrations of CO over time to vent areas at 100 m distance, 10 kg/s.

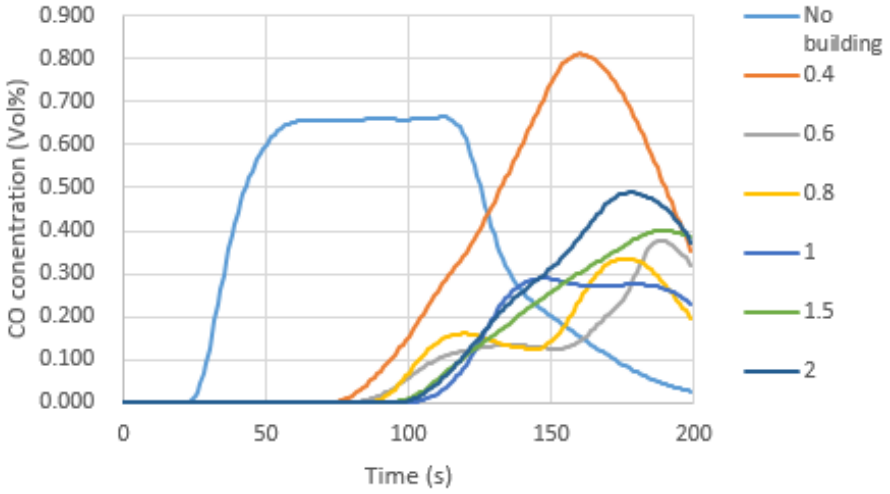

Figure 2.14 Concentrations of CO over time to vent areas at 200 m distance, 10 kg/s.

2.5. Concluding remarks

Firstly, the importance of selecting suitable accident models and their inputs were briefly discussed. The next part of this chapter was about the development of the indoor release model, which calculates gas flowrate and concentration during an indoor gas leak. If an accidental gas leak occurs inside a building, the effect of the building must be predicted. While CFD is a useful method that provides accurate prediction, it is only possible under sufficient resources to obtain accurate results. Without sufficient time to simulate, specific information to calculate, and human effort to organize, application of CFD in the field of process safety is limited. The indoor release model modifies the release flowrate and concentration of discharge flow for the dispersion calculation in much simpler terms. Validation and verification of the model for average indoor gas concentration had been done, demonstrating its accuracy. While the model may not predict complex mixing to the level of CFD, it provides compatible predictions with far less time and modeling parameters.

The additional studies carried out showed that under several occasions, the building could work as an effective mitigation method against hazardous gas leaks by diluting the concentration of gas released and restricts the dispersion area. Since residence time and spreading behavior are different between internal and external leaks, the emergency response should also consider the location of the leak. For mitigation purposes, the vent area should be above a specific limit to avoid negative effectiveness, while too large vent may result in low effectiveness as well. Also, large leaks require a small vent for high mitigation effectiveness while smaller leak requires a larger vent to maximize mitigation effectiveness. If

the target building is located in a larger chemical plant or near a populated area, the vent should be headed towards the direction, which causes the least damage in an immediate close range. Facilities and residences located at a distance are in low priority since the wind majorly determines the dispersion at a long-range.

Chapter 3. Interactive Process-Accident Simulation

3.1. Introduction

Human error is one of the main causes of industrial accidents. Many operator training simulators (OTS) have been developed with the aim of replacing existing plant safety training programs because they cannot provide efficient training to operators due to a lack of accurate data. In this chapter, the city gas pressure regulation station was simulated using interactive process-accident simulation to provide more accurate data. We simulate this by dynamic simulation assuming gas leakage occurs in urban gas pressure station. And the resulting dynamic hole information confirms the reliability of the result compared with the leakage calculated by other methods.

Using both processes and accident simulation can provide accurate data, since advanced research shows that linking the two simulations provide advantages on tracking the process, sizing safety areas, and quantifying damages.

3.2. Gas pressure regulation station case study

City gas pressure regulation station

City gas pressure regulation stations are where the gas supplied is depressurized, make them suitable to be distributed around the city. They are composed of a series of pipelines. Each line possesses one regulator valve and one safety suction valve. There are two types of regulation stations; Upstream, (Figure 3.1.) and downstream. (Figure 3.2.) It is the upstream station where gas is distributed to several lesser downstream pressure regulation stations. In order to do so, the pressure of the gas in the upstream should be higher than the downstream. The gas is first supplied to the upstream with 850kPa to be reduced to 600kPa in the upstream station. The gas pressure is reduced further down to 2kPa at the downstream station. Then the gas for distributed domestic and industrial uses around the city. If the regulator fails and the gas pressure remains above the designated pressure, leak accident may occur in the further down at the location of the numerous end-users. Hence, the potential risk is of this process is relatively high for its size, while the structure is simple. Therefore they are ideal for performing interactive simulation between process and accident. The steady-state simulation result is presented in Table 3.1.

Table 3.1 Steady state simulation result of upstream regulation station

Name	Vapor Fraction	Temperature [C]	Pressure [bar]	Molar Flow [kgmol/h]	Mass Flow [kg/h]	Liquid Volume Flow [m3/h]	Heat Flow [kcal/h]
1	1	0.00	8.34	4240.44	76950.99	241.47	-7.9E+07
2	1	0.00	8.34	1060.11	19237.75	60.37	-2E+07
3	1	0.00	8.34	1060.11	19237.75	60.37	-2E+07
4	1	0.00	8.34	1060.11	19237.75	60.37	-2E+07
5	1	0.00	8.34	1060.11	19237.75	60.37	-2E+07
6	1	0.00	8.34	1060.11	19237.75	60.37	-2E+07
7	1	-1.56	5.88	4240.44	76950.99	241.47	-7.9E+07
7-1	1	-1.72	5.63	4240.44	76950.99	241.47	-7.9E+07
8	1	-1.56	5.88	1060.11	19237.75	60.37	-2E+07
9	1	-1.56	5.88	1060.11	19237.75	60.37	-2E+07
11	1	-1.56	5.88	1060.11	19237.75	60.37	-2E+07
10	1	0.00	8.34	1060.11	19237.75	60.37	-2E+07
12	1	-1.56	5.88	1060.11	19237.75	60.37	-2E+07
13	1	0.00	8.34	1060.11	19237.75	60.37	-2E+07
14	1	0.00	8.34	1060.11	19237.75	60.37	-2E+07

Event tree analysis

Event tree analysis (ETA) may cover all the possible outcomes that may occur from a single event. The possible scenarios that will occur when the main regulator valve fails to regulate pressure to the level of desired pressure are covered through event tree analysis. Several consequences develop as to whether or not the safety suction valve worked, and how the relief valves operated. (Figure 3.3)

The most hazardous incident is a case of a gas leak that occurs when the main regulator valve malfunctions and safety suction valve of the regulator is not closed. In this case, the gas leak occurs due to overpressure within the pipeline. On the contrary, during the case when the pressure is dropped below the desired pressure, the worst and only possible undesired outcome is an emergency shutdown of the gas supply.

Since all gas pressure regulation stations are located indoors, the indoor release model developed in Chapter 2 would be useful to describe accident behavior of the potential scenarios.

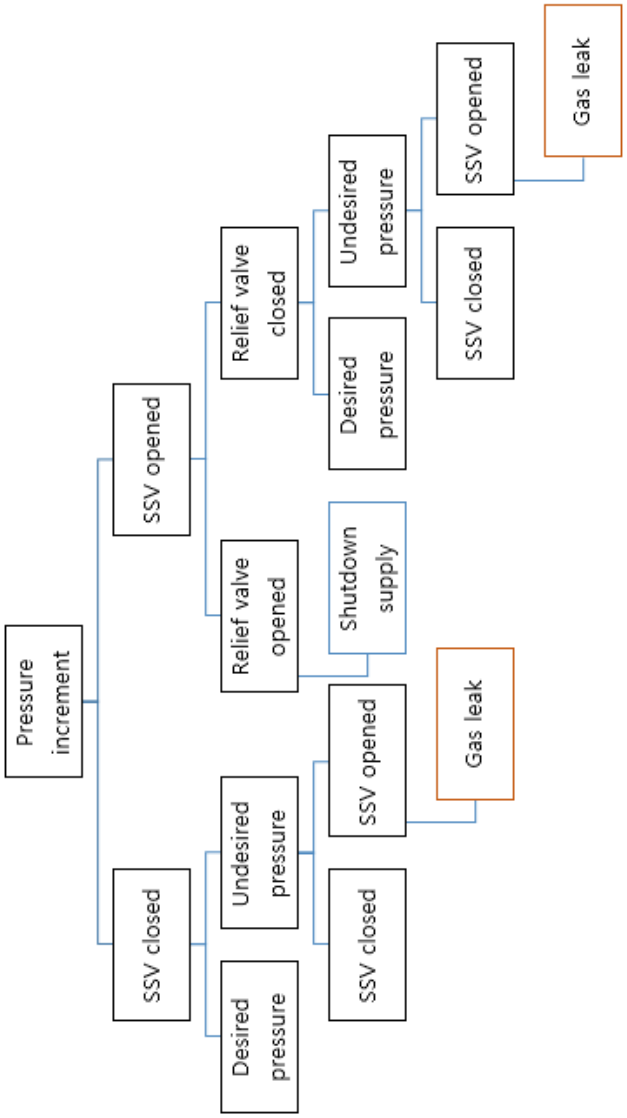

Figure 3.1 Event tree of pressure increase case

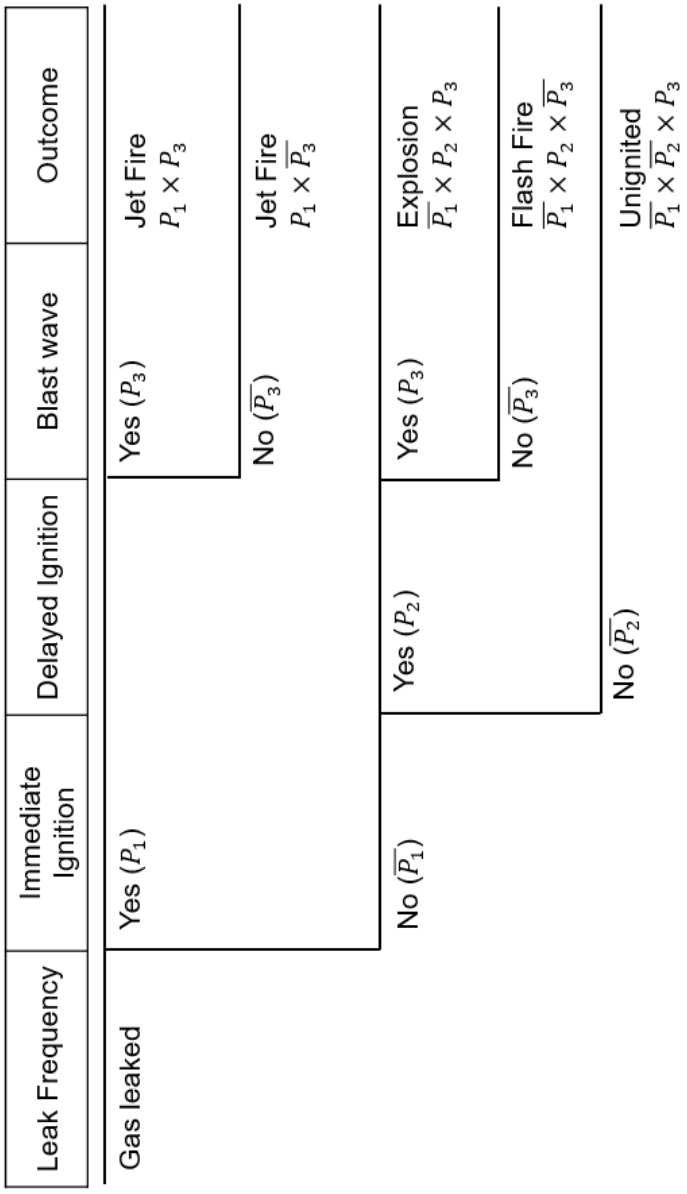

Figure 3.2 Event tree of a gas leak with the corresponding probability

Accident behavior study

Based on the event tree analysis performed, possible gas leak accidents were dynamically simulated using process data. The custom accident simulation was based on (2.4), and used the dynamic input obtained from simulation data that was transferred from real-time dynamic process simulation generated by Aspen HYSYS. The accident simulation was conducted simultaneously with HYSYS, following the process movement.

The results are presented in Table 3.2., and they were compared with results from Phast, one of the most widely used risk assessment software to verify the data. The difference between the two was within 1% when the discharge coefficient is set to the same value.

Table 3.2 Real-time dynamic simulation data for gas leak at regulation station

Pressure (kPa)	**Density (kg/m^3)**	**Cp/Cv**	**A1 (m^2)**	**A2 (m^2)**	**Chocked pressure (kPa)**	**Discharge rate (kg/s)**
31.8	0.244	1.28	1.96e-2	3.93e-4	-	0
608.7	4.683	1.3	1.96e-2	3.93e-4	332	0.265
513.0	3.946	1.3	1.96e-2	3.93e-4	280	0.224
410.0	3.145	1.3	1.96e-2	3.93e-4	224	0.178
515.9	3.844	1.3	7.85e-2	1.57e-3	282	0.883
579.5	4.300	1.3	7.85e-2	1.57e-3	317	0.991
657.0	4.886	1.3	7.85e-2	1.57e-3	359	1.125
827.1	6.176	1.3	7.85e-2	1.57e-3	451	1.421

3.3. Concluding remarks

In this study, the development of a plant interactive simulation model of city gas regulating station was conducted. The developed model was designed to use process data from the simulation as an input. The interactive simulation technique is expected to identify unprecedented risk and perform with higher effectiveness when the process becomes more complex, so independent risk assessment attempts become more challenging. The result of the developed model was verified with conventional QRA software to confirm its liability. It was concluded that the models implemented for the accident simulation were accurate and dynamic calculation based on the process stream data. The fundamental technique developed in this Chapter will be used in the following Chapter 4.

Chapter 4. Process Design with Inherent Safety

4.1. Introduction

So far, techniques and methods that can be used during the risk assessment for the chemical process were presented and discussed. QRA plays an important role both in the process design and safety in order to ensure the degree of safety for the designed process. However, it often became both time and cost consuming procedure because it had to be undergone multiple times until the risk criteria are met. To avoid this repetitive work, the risk could be handled during the design stage. This approach of preventing risk in the preliminary design stage from exceeding the limit is called as the inherent safety approach.

Inherent safety approach is one of the four fundamental systematic strategies (inherent, passive, active, procedure) to achieve safety in the chemical process.[24] This approach makes alterations to the design or the materials used in the process, decreasing risk by removing potential causes, and avoiding the design that might develop into severe consequences in case of an accident. Because of its nature, the inherent safety approach is most yields the best results when applied during the preliminary design stage.[25] Unlike other methods, this approach aims to avoid and reduce hazards by designing a safer process rather than preventing them through active control measures.[26] There are six fundamental principles for designing an inherently safe process: Intensification, Substitution, Attenuation, Limitation of effects, Simplification, Error tolerance. By following these principles, the inherent safety approach could reduce either the magnitude or the likelihood of an accident so that it would require fewer layers of protection.[24] Since mitigation require high-level technical expertise and both monetary and

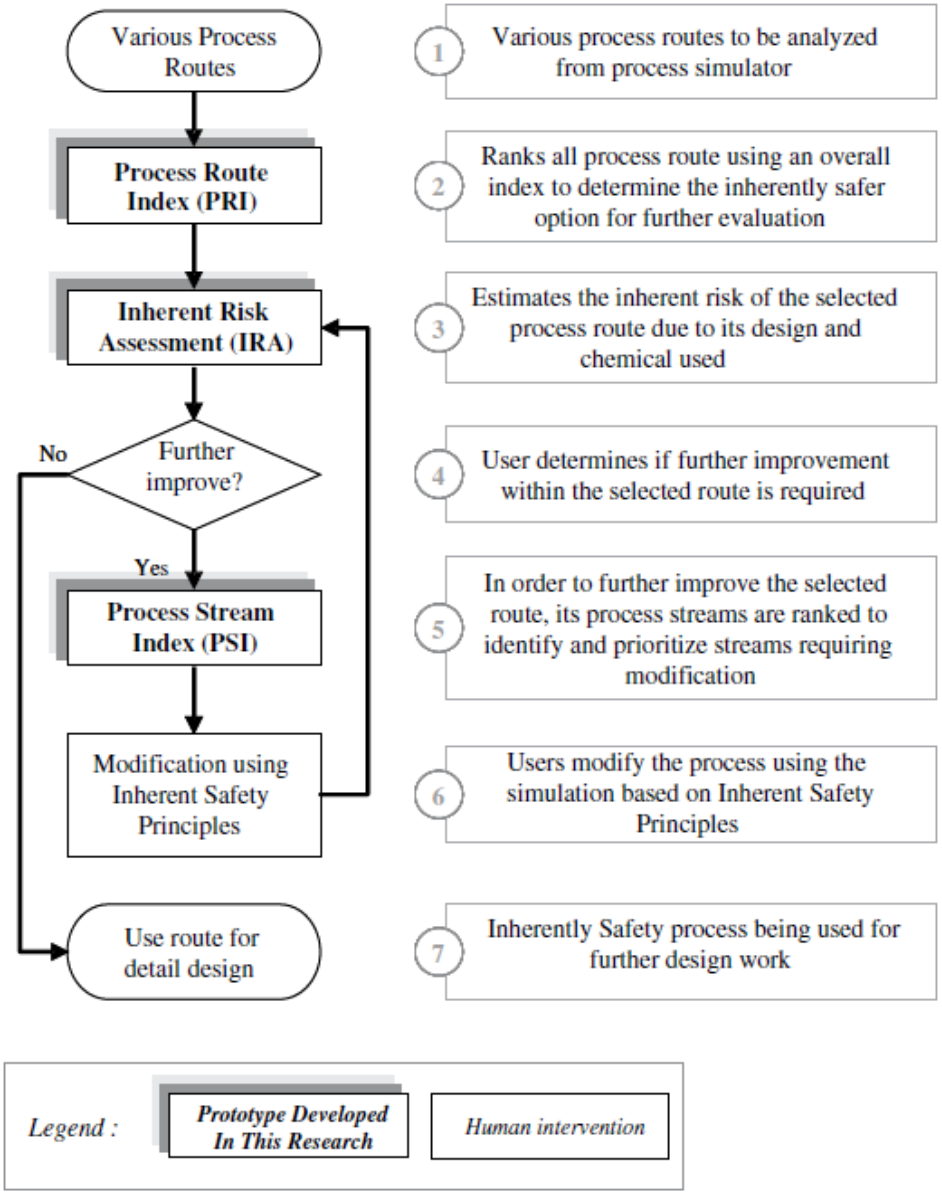

Figure 4.1 Design Modification Method using safety indexes proposed by Leong and Shariff [44]

time investments throughout plant life, the process designed by the inherent safety approach is relatively safer at lower capital and operating costs.[27]

There were attempts to integrate risk into process design and optimization. Shah et al.[28] firstly demonstrated the value of a multi-objective approach at the conceptual stage for energy efficiency and hydrocarbon inventory related to the inherent safety. Eini et al. proposed an optimization procedure that integrates both processing and accident costs from consequence modeling techniques through defining an objective function as the sum of accident costs and plant lifecycle processing costs.[29] Later Eini et al. developed a multi-objective optimization framework for simultaneously minimizing each cost for a simple refrigeration cycle.[30]

The majority of the attempt to design an inherently safer process involves safety indexes.[31, 32, 33, 34] The first safety index is suggested as an indication to quantify safety by Edwards and Lawrence in 1993 [35], then followed by Heikkilä et al. in 1996 [36]. There are different types of safety indexes that require different data and aim different goals, and inherent safety indexes require chemical and process data from the early design stage to be used as an inherent safety approach. Researchers have considered implementing safety indexes into multi-objective optimization, using the former as the objective of the latter. The aim of these multi-objective optimizations was to achieve both the economically feasible and inherently safer process. Rangaiah and Bonilla-Petriciolet optimized a cumene process for multiple objectives with an economic objective and I2SI safety index using an NSGA-II method in their book.[37] Athar et al. developed a methodology that an external risk from critical equipment identified by PSI safety index and

process economics model is coupled with Aspen HYSYS to design optimal process.[38]

Meanwhile, relatively few studies are performed for the latter one using consequence modeling as it requires complex theories and equations consuming high computation cost and a long time. Shariff et al. developed an explosion consequence evaluation module called integrated risk estimation tool (iRET) based on TNT equivalence method with TNO correlation one.[39] Similarly, Shariff and Zaini developed a toxic release consequence analysis tool (TORCAT) [40], and later Shariff et al. developed an inherent fire consequence estimation tool (IFCET) to assess the boiling liquid expanding vapor explosion (BLEVE) scenario.[41]

The aforementioned studies contributed a lot to the inherent safety design in that they formulated a superstructure for the target process and perform a multi-objective optimization considering inherent safety using inherent safety indexes or consequence modeling. First two references evaluated the risk through simplified consequence modeling. However, they decided only whether the parallel n trains with 1/n capacity or a single train with full capacity would be better without considering the thermodynamic efficiency in the heat exchanger, which is the critical issue in the liquefaction process.[42, 43] Also for the last two references, as they assessed the inherent safety level of the separation structure using some indexes which cannot adequately consider the accidental situation, the optimization results showed that more distributed structures are prioritized over thermally coupled one in the safety manner even though the more distributed the system is, the more prone it is to be exposed to the accidental releases.[29, 30] Due to those limitations, the conclusions are hard to provide reasonable guidelines

for the process designers.

In this chapter, a new decision-making scheme aiming to find the optimal solution between the economic feasibility and the inherent safety was proposed and compared. The repetitive nature of the conventional approach is reduced by simultaneously considering both factors through using the actual risk as to the second objective function by incorporating risk assessment methodology into multi-objective optimization. The developed approach is applied to designing an optimal natural gas liquefaction processes as they could verify the effectiveness of the proposed method in that the feasible operating range for the pressure, flowrate, and composition of the refrigerant cycles they use are broad enough to see the trade-off relation between economic feasibility and safety. Generally, with higher pressure at which the cycle is discharged from the compressor, less flowrate of the cycle and smaller heat transfer area are required for the same liquefaction but with higher hazards in case of an accident. The structure of a liquefaction process could vary with respect to the refrigeration cycles it uses. Three structures are selected including a single-stage mixed refrigerant process (SMR), a pre-cooled process without phase separators (Precooled), or a dual-mixed refrigerant process with the pre-cooling refrigerant evaporated at double pressures (DMR). These processes share similar heat transfer structures in producing the same amount and quality of product LNG, only different in the number of multi-stream heat exchangers and/or that of refrigerant cycles. Due to this similarity, it could approximate the superstructure of a liquefaction process by expanding its structure from SMR to DMR. Then the proposed approach could give reasonable guidelines to the designer who wants to decide not only the optimal design conditions.

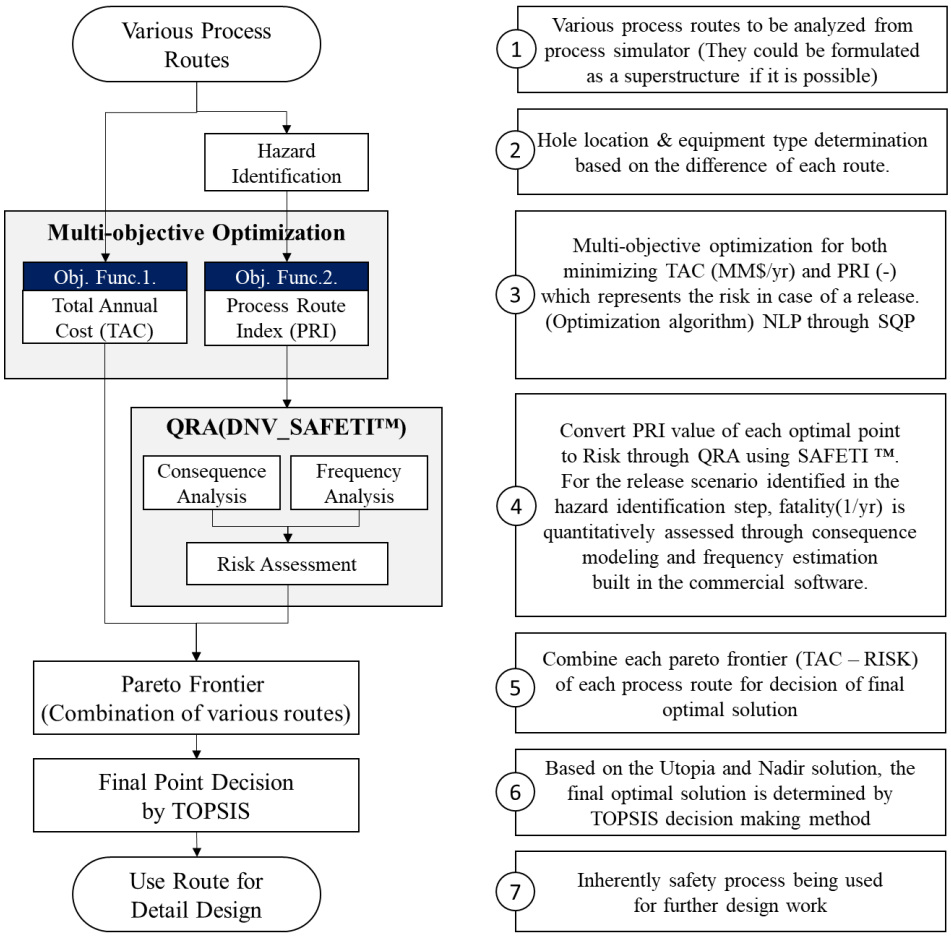

Figure 4.2 The framework of decision-making scheme using TAC and PRI as objective functions [45]

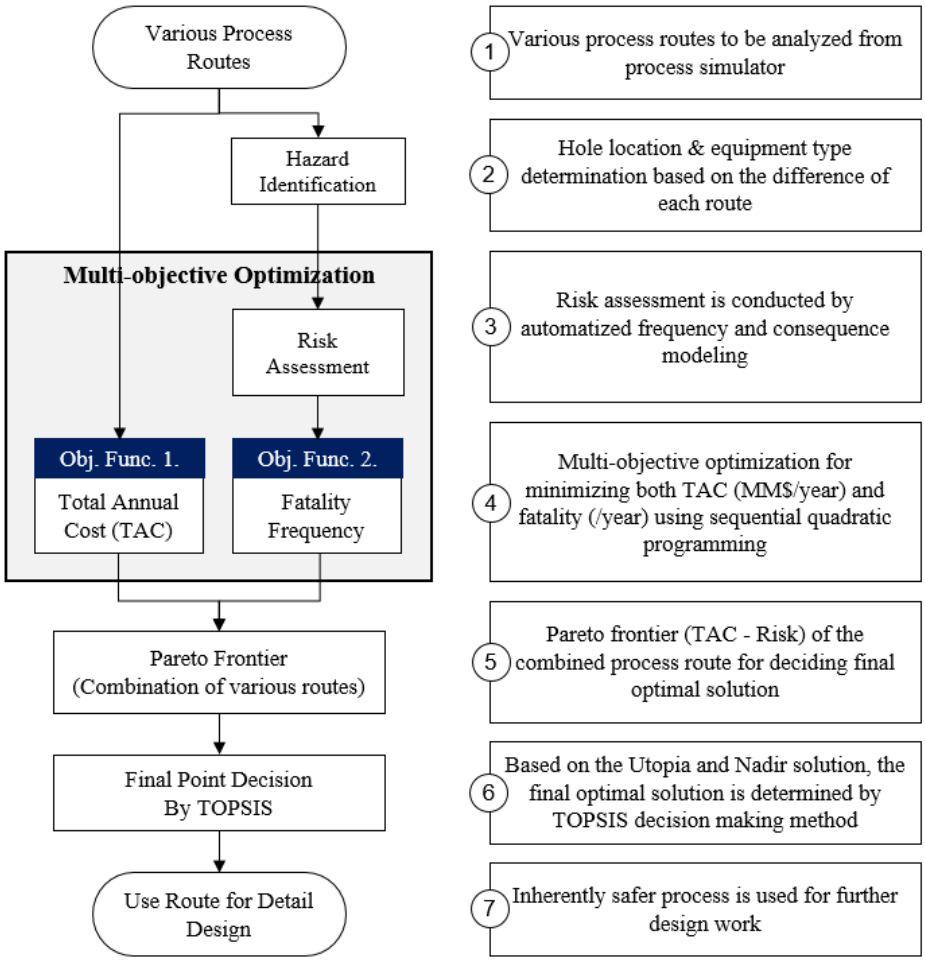

Figure 4.3 The framework of decision-making scheme with integrated risk assessment

4.2. Process description

Natural gas liquefaction processes used in this study are designed based on three processes of 3 metric tonnes per annum (mpta), shown in Figures 4.4, 4.5, and 4.6. The physical conditions of the feed natural gases are listed in the corresponding Tables 4.1, 4.2, and 4.3. The feeds are mostly composed of light hydrocarbons and nitrogen, and the MR stream conditions are optimized to maximize the thermodynamic efficiency of the process.

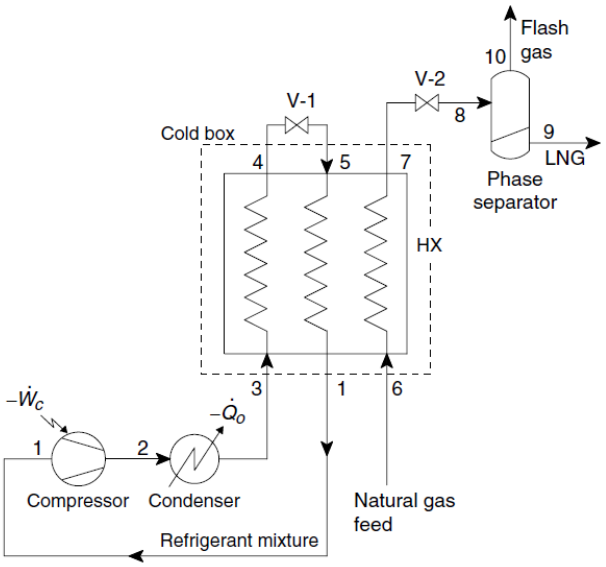

Figure 4.4 Single-stage mixed refrigeration process [46]

Table 4.1 Main stream data for 3mtpa SMR process [45]

		NG FEED	Mixed Refrigerant		LNG (3mtpa)
			Condenser outlet	V-1 outlet	
Pressure	bar	65	17.6	1.6	1
Temperature	K	300.00	310.00	110.00	107.18
Flowrate	kg/s	114	541	541	106
	kmol/h	22549	49687	49687	21001
Composition					
N2	mol/mol	0.0400	0.0680	0.0680	0.0162
C1	mol/mol	0.8750	0.2291	0.2291	0.8926
C2	mol/mol	0.0550	0.3294	0.3294	0.0591
C3	mol/mol	0.0210	0.0904	0.0904	0.0223
nC4	mol/mol	0.0050	0.0494	0.0494	0.0054
iC4	mol/mol	0.0030	0.0000	0.0000	0.0032
iC5	mol/mol	0.0010	0.2333	0.2333	0.0011

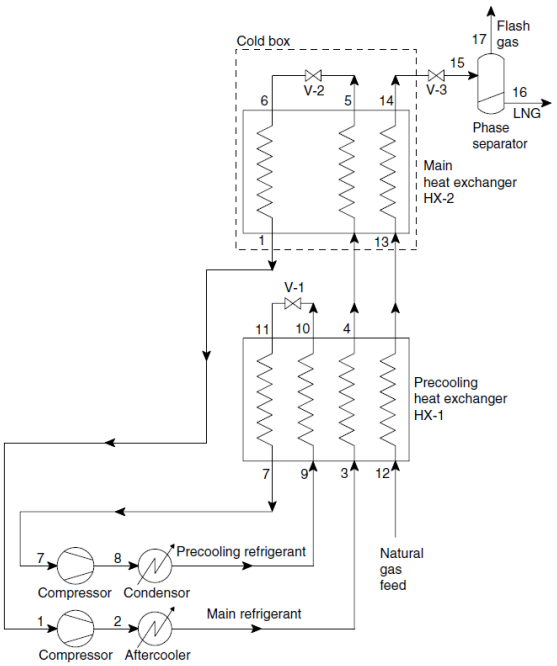

Figure 4.5 Precooled process [46]

Table 4.2 Primary stream data for 3mtpa Precooled process [45]

		NG FEED	Mixed Refrigerant 1		Mixed Refrigerant 2		LNG
			Cond outlet	V-2 outlet	Cond outlet	V-1 outlet	
Pressure	bar	65.0	23.7	1.8	17.3	1.6	1.0
Temperature	K	300.00	310.00	108.95	310.00	219.56	107.18
Flowrate	kg/s	114	197	197	326	326	106
	kmol/h	22549	26030	26030	25113	25113	21001
Composition							
N2	mol/mol	0.04	0.0768	0.0768	0.0000	0.0000	0.0162
C1	mol/mol	0.875	0.3447	0.3447	0.0000	0.0000	0.8926
C2	mol/mol	0.055	0.4228	0.4228	0.2947	0.2947	0.0591
C3	mol/mol	0.021	0.1557	0.1557	0.2264	0.2264	0.0226
nC4	mol/mol	0.005	0.0000	0.0000	0.4789	0.4789	0.0054
iC4	mol/mol	0.003	0.0000	0.0000	0.0000	0.0000	0.0032
iC5	mol/mol	0.001	0.0000	0.0000	0.0000	0.0000	0.0011

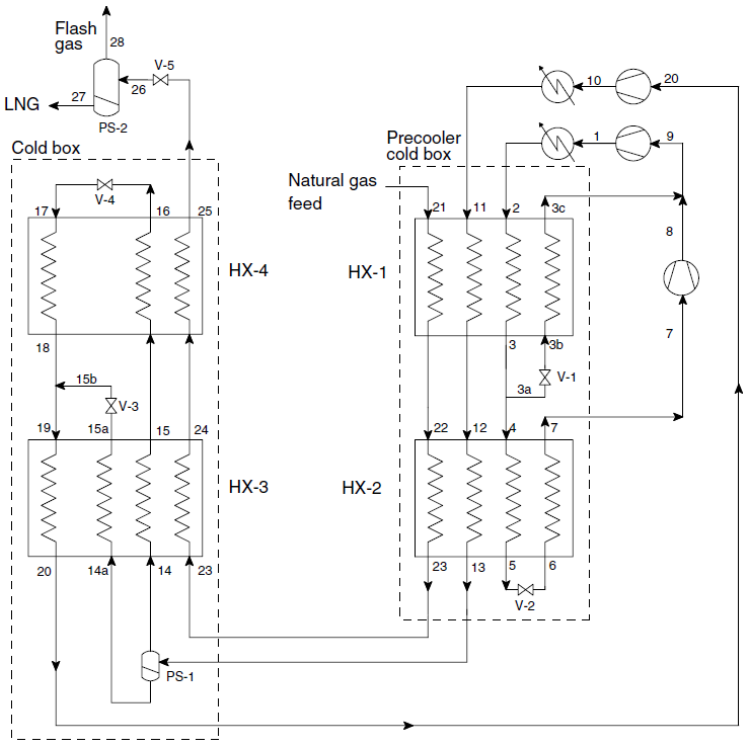

Figure 4.6 Dual mixed refrigerant process [46]

Table 4.3 Primary stream data for 3mtpa DMR process [45]

		NG FEED	Mixed Refrigerant 1			Mixed Refrigerant 2			LNG
			Cond outlet	V-1 outlet	V-2 outlet	Cond outlet	V-3 outlet	V-4 outlet	(3mtpa)
Pressure	bar	65.0	19.4	5.0	1.6	31.4	3.0	3.0	1.0
Temp	K	300	310	254	220	310	152	113	107
Flowrate	kmol/h	22549	31389	18802	12587	30327	18197	12130	21001
Composition									
N2	mol/mol	0.040	0.00	0.00	0.00	0.064	0.02	0.14	0.02
C1	mol/mol	0.875	0.00	0.00	0.00	0.43	0.27	0.69	0.89
C2	mol/mol	0.055	0.27	0.27	0.27	0.39	0.53	0.16	0.06
C3	mol/mol	0.021	0.54	0.54	0.54	0.12	0.19	0.01	0.02
nC4	mol/mol	0.005	0.19	0.19	0.19	0.00	0.00	0.00	0.005
iC4	mol/mol	0.003	0.00	0.00	0.00	0.00	0.00	0.00	0.003
iC5	mol/mol	0.001	0.00	0.00	0.00	0.00	0.00	0.00	0.001

4.3. Design optimization

The proposed decision-making scheme in Figure 4.3 assesses the risk prior to the optimization by applying rigorous custom modeling. TAC is the first objective function, and instead of calculating individual risk separately after the process optimization, the risk for each case is calculated and designated as the second objective function. This methodology should cover the entire process route and consider every equipment, since focusing only on the critical equipment can lead to neglecting certain risk that may prove disastrous in the optimal solutions.

Cost estimation

As noted in the previous section, the first objective function in multi-objective optimization is TAC. Fixed and operational costs can be obtained after defining process routes. Yearly operating costs and initial capital costs are in different dimensions and should be converted to match one another. In the case study, the TAC of the processes was obtained by calculating capital expenditures (CapEx) and operating expenditures (OpEx), converting the former into annual expenditure.

Risk estimation

The second objective function is the risk of the process route. Since the integrated risk assessment in the optimization procedure follows the conventional approach, individual risk for an event can be expressed as a product of consequence and likelihood.

$$(Risk)_{Event} = (Consequence)_{Event} \times (Likelihood)_{Event} \quad (4.1)$$

The likelihood is the probability of occurrence, multiplication of equipment failure frequency and the event probability which can be obtained from ETA, simplified in Figure 3.4.

$$(Likelihood)_{Event} = (Frequency)_{Failure} \times (Probability)_{Event} \quad (4.2)$$

Therefore, the overall risk of the process can be expressed in (4.3). For this study, fatality frequency (year^{-1}) was selected as a risk value.

$$Risk = \sum[(Consequence)_{Event} \times (Frequency)_{Failure} \times (Probability)_{Event}] \quad (4.3)$$

Ignition and explosion probabilities are obtained from the review of literature data.[47] By multiplying successive probabilities, each of the final event probability can be obtained. The sum of the probabilities that originate from a single event should be 1.

Equipment failure frequencies are standardized in Table 4, which are retrieved from the data directory by HSE [48] and Oil & Gas Producers [49]. Equipment other than heat exchangers were analyzed to conclude centrifugal compressors and valves along pipelines are the main weak points that may cause accidents. Since every failure frequency was considered independently in this study, the

more equipment the process uses, the failure probability generally increases, resulting in increased risk.

The consequence is calculated through corresponding consequence models. Discharge and other consequence models are selected from validated, reliable models from CCPS [50], and TNO's Yellow book [51].

For damage calculation, probability unit (Probit) functions account for the harm of an exposed population. The fatality rate of personnel exposed to hazardous agents like toxic material or thermal radiation can be expressed as,

$$Y = a + b \ln X \tag{4.4}$$

Where a, and b are characteristic constants that are decided experimentally, and X is a variable of the intensity of hazardous agents received to an exponent and the duration of exposure. Y is a probit that represents fatal probability. From Pareto estimation suggested by Finney, the probability of fatality is 99.9% when the probit value is 8.09, 50% when 5.00, and 1% when 2.67 [52], and the range is selected based on the recommendation given by HSE.[53]

$$Y = -37.23 + 2.56 \ln(t \times I^{\frac{4}{3}}) \tag{4.5}$$

For fire, X is thermal dose($= t \times I^{\frac{4}{3}}$), where t is exposure time (s), and I_T is thermal radiation (kW/m^2). The exposure time was set to 300 seconds, which is also the time to evacuate to the shelter.

For the explosion, we used Trinitrotoluene (TNT) equivalent method, assuming 4.184 MJ of energy is produced per kilogram of TNT. TNT equivalence of the released material is set to 0.03.[54] The fatality is determined by overpressure using probit functions.

$$Y = -46.1 + 4.82 \ln P_s \quad (4.6)$$

where P_s is overpressure expressed in kPa, caused by the explosion.

The frequency, probability, and consequence data and models are embedded in gProms Processbuilder v1.1. when the optimization is performed. Even though the three processes are different, the similarity between them enables the same frequency and consequence models to be used during the preliminary design stage.

Table 4.4 Equipment failure frequency data (per year)

	Pin Hole (10mm diameter)	Small Hole (50mm diameter)	Large Hole (100mm diameter)	Rupture
Actuated valve, 6 inches	4.9×10^{-4}	5.7×10^{-5}	3.2×10^{-5}	1.6×10^{-5}
Actuated valve, 12 inches	1.1×10^{-4}	1.8×10^{-5}	1.3×10^{-5}	1.6×10^{-5}
Centrifugal compressor	8.4×10^{-3}	8.7×10^{-4}	3.6×10^{-4}	2.9×10^{-6}

Solving the multi-criteria problem

Since the two objective functions we defined compete with each other, there is no unique solution that optimizes both objectives simultaneously. An optimal solution in multi-objective optimization is a solution where there is no other feasible solution that improves at least one objective function value without deteriorating any other objective. For TAC and fatality frequency used in this study, each objective functions cannot be optimized further without undermining another. Therefore, a weighted sum approach was used to find Pareto optimality from this multi-criteria decision making (MCDM) problem. The weighted sum approach allows us to solve this multi-objective optimization problem as a series of single-objective optimization problems like Equation 4.7.[55]

$$\min \sum_{i=1}^{k} \omega_i f_i'(x) \qquad (4.7)$$
$$\text{s.t. } x \in \Omega$$

where assigned scalar weights ω_i is $\omega_i \geq 0, \forall i = 1, \ldots, k$ and $\sum_{i=1}^{k} \omega_i = 1$, while k = 2. $f_i'(R^n \to R)$ is the i-th normalized objective function $f_i(R^n \to R)$ and $\Omega(\in R^n)$ is the feasible region.

Each objective functions are normalized by the differences of optimal values in the Nadir (negative-ideal) and Utopia (positive-ideal) points that give the length of the intervals where the optimal objective functions vary within the Pareto optimal set.

$$z_i^U = f_i\left(x^{[i]}\right) \quad where\ x^{[i]} = argmin_x\{f_i(x): x \in \Omega\} \tag{4.8}$$

$$z_i^N = max_{(1\leq j\leq k)}\left(f_i\left(x^{[j]}\right), \qquad \forall i = 1, \dots, k \right. \tag{4.9}$$

$$f_i'(x) = \frac{f_i(x) - z_i^U}{z_i^N - z_i^U} \tag{4.10}$$

where z^U, z^N are Utopia and Nadir points, respectively.

Decision making of a final optimal solution

Every solution sets on the Pareto frontier has the potential to be selected as the optimal solution. Generally, this has to be determined by a restriction on the side of process safety. However, it is too early to formulate exact risk value during this stage of the process design, since the process safety will most likely to fluctuate as the design develops. Therefore, the final optimal solution is determined by using the technique for order of preference by similarity to ideal solution (TOPSIS) method. As one of the most widely used methods to solve the MCDM problem,[56, 57] TOPSIS method determines the solution by the closeness to the ideal solution. The Utopia point and Nadir point can be expressed as $z^U = (v_1^+, v_2^+)$, $z^N = (v_1^-, v_2^-)$ respectively, where 1 and 2 each denote the value of each objective functions. Then the separation of alternatives (v_{i1}, v_{i2}) from the Utopia and Nadir solutions is given as Equation 4.11 and Equation 4.12, and the relative closeness of *i*-th alternative with respect to the Utopia solution, CL_i, is defined as Equation 4.13.

$$d_i^+ = \sqrt{\sum_{j=1}^{n}(v_{ij} - v_j^+)^2}\ ,\ i = 1, \dots, m \tag{4.11}$$

$$d_i^- = \sqrt{\sum_{j=1}^{n}(v_{ij} - v_j^-)^2}\ ,\ i = 1, \dots, m \tag{4.12}$$

$$CL_i = \frac{d_i^-}{d_i^- + d_i^+}\ ,\ i = 1, \dots, m \tag{4.13}$$

where m is the number of optimal points in the Pareto frontier set.

The overall combined Pareto frontier is presented in Figure 4.7. The closer the solution to the Utopia point, it is more optimal. Among the solutions presented in Pareto frontier, the solution closest to the Utopia point is set 11 of Table 4.5, that TAC is 620 MM$/year, and the fatality frequency is 0.00144/year. (SMR, Y = 0.8105) and the alternative solutions can be obtained by ranking the relative closeness in descending order. The specification of the optimal objective functions is given in Table 4.6.

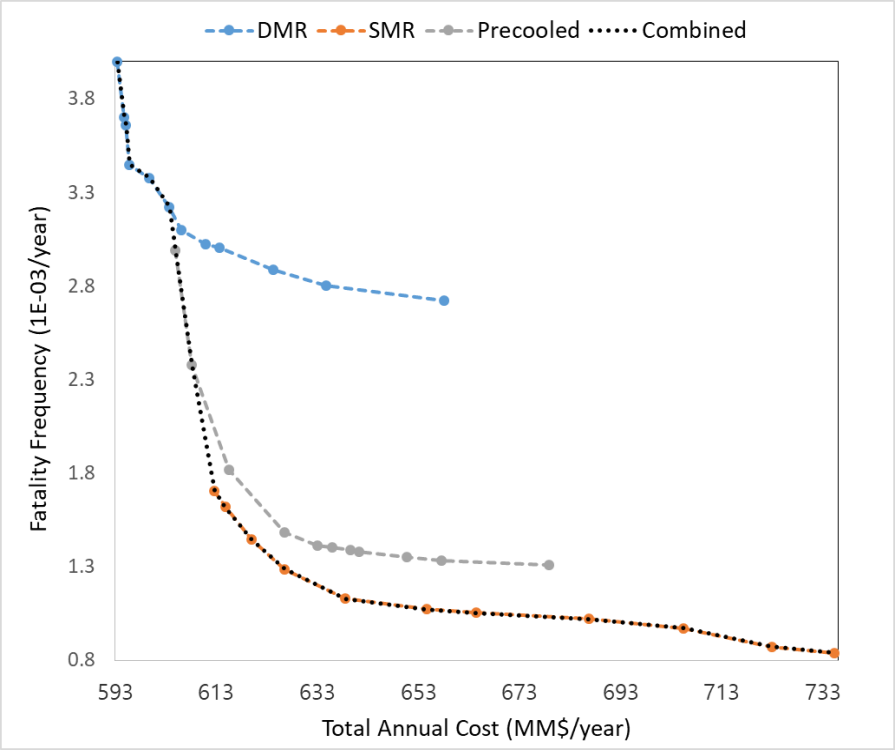

Figure 4.7 Combined Pareto frontier

Table 4.5 Combined Pareto frontier and the final optimal solution with TOPSIS

Process	i	Actual		Normalized		TOPSIS		
		TAC	F.F*	F1**	F2**	d+	d-	CL
DMR	1	594	4.00	0.00	1.00	1.00	1.00	0.500
	2	595	3.70	0.01	0.91	0.91	0.99	0.523
	3	595	3.66	0.01	0.89	0.89	0.99	0.527
	4	596	3.45	0.02	0.83	0.83	1.00	0.547
	5	600	3.38	0.04	0.80	0.81	0.98	0.548
	6	604	3.22	0.07	0.76	0.76	0.96	0.558
Precooled	7	605	2.99	0.08	0.68	0.69	0.97	0.586
	8	608	2.38	0.10	0.49	0.50	1.03	0.675
SMR	9	613	1.71	0.14	0.27	0.31	1.13	0.787
	10	615	1.62	0.15	0.25	0.29	1.14	0.797
	11	620	1.44	0.19	0.19	0.27	1.15	0.810
	12	627	1.29	0.23	0.14	0.27	1.15	0.808
	13	639	1.13	0.32	0.09	0.33	1.14	0.774
	14	655	1.07	0.43	0.07	0.44	1.09	0.713
	15	664	1.05	0.50	0.07	0.50	1.06	0.677
	16	687	1.02	0.66	0.06	0.66	1.00	0.603
	17	706	0.97	0.79	0.04	0.79	0.98	0.553
	18	723	0.87	0.91	0.01	0.91	0.99	0.521
	19	735	0.84	1.00	0.00	1.00	1.00	0.500

*FF: Fatality frequency, [1/year] * 1E-03

** F1, F2: Normalized objective functions; 1: TAC, 2: Fatality frequency

Table 4.6 The final solution

i	CAPEX (MM$/year)	OPEX (MM$/year)	Fatality Frequency(1E-03/year)		
			Compressor	V-1	V-2
11	277.7	342.5	1.265	0.03811	0.1412

It can be observed from the combined Pareto frontier of three processes that it is more economically feasible in order of DMR, Precooled, SMR process while it is safer in order of SMR, Precooled, and DMR process. This confirms that economic feasibility and the process safety are competing against each other, and the trade-off between the two exists.

From the specifications of the final solution of SMR, major potential risks is identified in Table 4.7. It is noted that the explosion is the riskiest accident. Furthermore, compressor C-1 poses the most threat to process safety. The explosion from the compressor accounts for the majority of the overall risk particularly. As the major equipment, type of accident and risk are identified as the result of the preliminary design optimization, active safety approach should be focused on the compressor and preventing the explosion, decreasing safety assessment effort in the later design stage.

Table 4.7 Major potential risks in the final solution

Order	Equipment	Accident type
1	Compressor C-1	Explosion
2	Valve V-2	Explosion
3	Compressor C-1	Jet Fire
4	Valve V-1	Explosion

Comparison with the other methods

The risk calculation method we used in this study is different from the method used by commercial software Phast and SAFETI, results different outcomes. For example, SAFETI used assumed static inventory when calculating the consequence, which the current modeling did not, since the data is obtained from respective flow data. Due to this gap, the scale of the final risk value is also different compared to other works. However, while direct comparison between the risk result is improbable due to this difference, the optimal solution is still can be obtained and compared since every data were normalized prior to the calculation.

The optimal solution for the methodology presented in Figure 4.2 can also be obtained in the same manner from Pareto frontier set presented in Lee et al. [45]. Lee et al.[45] used PRI as one of the objective functions for representing the risk for its applicability to processes of flammable materials. The optimal solution that was obtained from using safety indexes is 627 MM$/year, where respective values are, from this research, 0.00129/year, and Y = 0.08083. Furthermore, they are set of a few indexes that can be incorporated into process design simulator and hazardous equipment used in the process can be identified from PSI analysis. The solution obtained from here is a near-optimal solution; close enough to be the optimal solution of the current study if there was a slight shift of the Utopia or Nadir points. However, the previous study couldn't found the current solution, since according to the previous assessment, it wasn't on the Pareto frontier. (Figure 4.8) Instead, the Precooled process on the Pareto frontier of 620 MM$/year when the multi-objective optimization was conducted with PRI. Therefore, it can be concluded that while two results are similar, the risk-using

proposed decision-making scheme identified the solution that could not be found by the method that uses PRI.

$$PRI = \left(\overline{mass\ heating\ value}\right) \times \left(\overline{fluid\ density}\right) \times (\overline{pressure}) \times \overline{\Delta FL_{mix}})/10^8 \tag{4.14}$$

$$PSI = \frac{mass\ heating\ value}{\overline{mass\ heating\ value}} \times \frac{fluid\ density}{\overline{fluid\ density}} \times \frac{pressure}{\overline{pressure}} \times \frac{\Delta FL_{mix}}{\overline{\Delta FL_{mix}}} \tag{4.15}$$

In Figure 4.9, Pareto Frontier comparison between PRI, derived from process stream data, and fatality frequency, derived from risk assessment based on PRI-based optimization result by Lee et al.[45] is presented. The difference between the two values indicates direct risk assessment can expect more accurate results.

Another comparison can be made between the risk-based decision-making scheme and the safety index-based methods from Process Stream Index (PSI).[58] Similar to PRI, PSI quantifies the risk of individual streams while PRI quantifies the risk of the whole process. It was used to determine the most critical streams in the process during the preliminary design stage, as presented in Figure 9. While the prediction made by PSI is not quantitatively accurate, it accurately predicted which stream would possess the highest risk. However, the same cannot be said for the second or lower priority streams, and the risk assessment was more accurate.

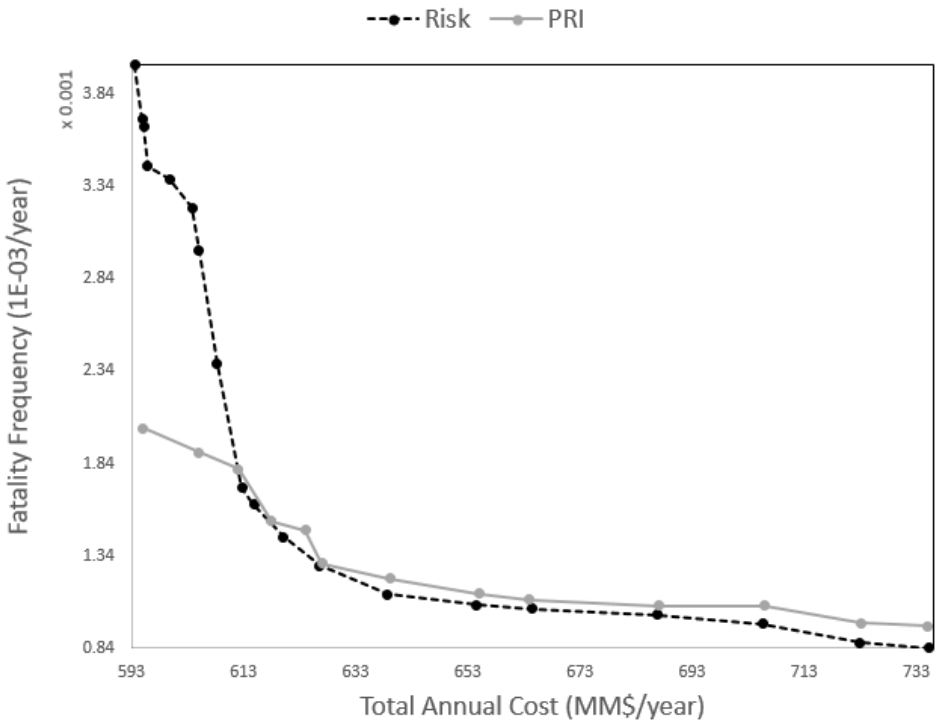

Figure 4.8 Comparison of Pareto Frontiers between risk-based method and PRI-based method

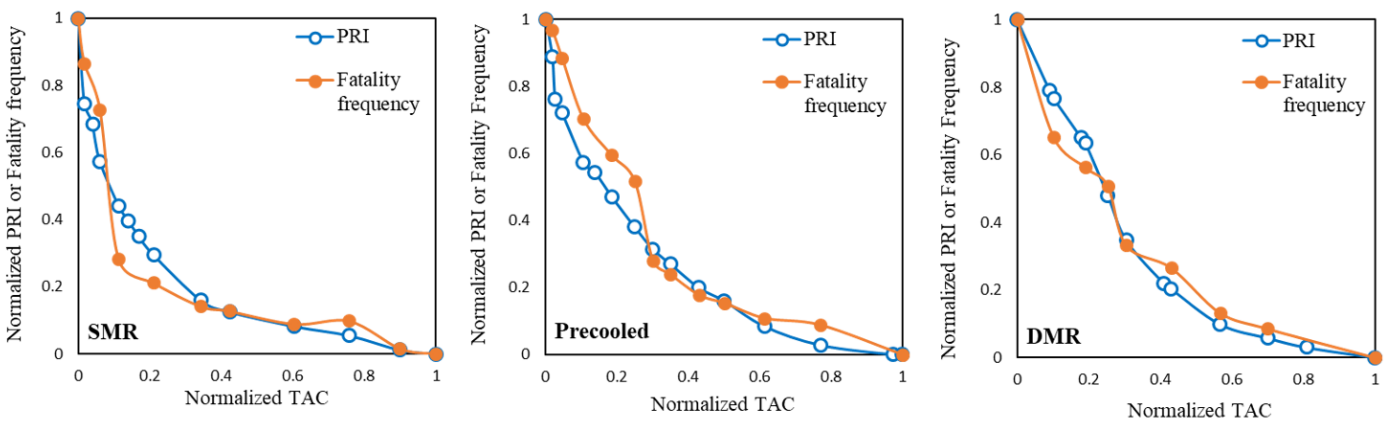

Figure 4.9 Pareto Frontier of PRI and Fatality frequency [46]

4.3. Concluding remarks

A new process design decision-making method for optimizing both the economic feasibility and the risk was proposed in this study. The proposed method was applied to the natural gas liquefaction processes of SMR, Precooled and DMR process, and found Pareto optimal set using weighted sum approach and TOPSIS method, with the total annual cost and the fatality frequency as objective functions. Lastly, the final optimal solution was found with the SMR process with TAC of 620 MM$/year and fatality frequency of 1.44E-03/year, and it is compared with another decision-making scheme that used Process Route Index.

The proposed method does not replace the necessary risk assessment procedure; it only reduces the further design effort by designing an inherently safe process. Like many other studies that conduct risk assessment during the early, preliminary design stage, detailed risk calculation, and rigorous safety evaluation were inhibited due to the lack of design data. The more rigorous, detailed risk-based approach can only be available after the detailed design is complete.

Furthermore, due to rigorous modeling within the problem, it requires a certain level of computational power. If the power is insufficient to perform complex calculations or one cannot find Pareto optimality during the procedure, one can alternately convert the risk into risk expenditure and combine the competing two objective functions into the single objective function. This approach is identical to a normalized 50 : 50 weighted sum approach, which calculates a single mathematical objective while the proposed method in the study calculates every combination in the weighted sum approach. This may lead to unexpected results due to the neglect of weight difference might yield a solution that is accident-proof

yet too expensive, or have minimum economic weight yet too risky. Therefore one should give the conditions that will limit the extremes, e.g., the risk expenditure not to exceed the safety criteria. These two limitations are needed to be overcome in the future.

Chapter 5. Conclusion

The risk-based design of chemical processes is studied in this thesis. The risk-based methodologies are proposed in the form of microscopic consequence modeling, process-accident interactive simulation, and risk-based multi-objective optimization in order to solve the problem of how to manage the risk fundamentally during the general procedures of process design.

The consequence models used in risk assessment procedures were conducted in Chapter 2 with development and validation of the indoor release model. In Chapter 3, a process-accident interactive simulation was studied using consequence models presented in Chapter 2. Case study of city gas pressure regulation station was performed, and the results were compared with conventional QRA software to verify the validity of the interconnection between the process simulation and the accident simulation and usage of dynamic process data into the consequence analysis. Lastly in Chapter 4, the new methodology was applied for designing optimal operating conditions of three different natural gas liquefaction processes considering the inherent safety and economic feasibility. Pareto frontier was presented combining three processes, and it was decided that the SMR process with the TAC of 620 MM$/year and the fatality frequency of 0.00144/year has the priority over the solutions.

Nomenclature

Acronyms and Abbreviations

BLEVE	Boiling Liquid Expanding Vapor Explosion
CFD	Computational Fluid Dynamics
CSB	U.S. Chemical Safety and hazard investigation Board
DMR	Dual-Mixed Refrigerant process
HAZOP	HAZard and OPerability study
H&MB	Heat and Material Balance
LNG	Liquified Natural Gas
MCDM	Multi-Criteria Decision Making
NSGA-II	Nondominated Sorting Genetic Algorithm II
OTS	Operator Training Simulator
PFD	Process Flow Diagram
PHA	Process Hazard Analysis
Precooled	Pre-cooled process without phase separators
PRI	Process Route Index
Probit	Probability unit
PSI	Process Stream Index
QRA	Quantitative Risk Assessment
SMR	Single-stage Mixed Refrigerant process
TNT	Trinitrotoluene
TOPSIS	Technique for Order Preference by Similarity to an Ideal Solution

Variables

A	Area (m^2)
$C_{A,max}$	Maximum concentration with a building with vent area of A
C_D	Discharge coefficient
$C_{No,max}$	Maximum concentration with no building
c	Interior molar concentration
c_d	Interior molar concentration at the end of the release
c_i	Interior molar concentration at time step i
c_o	Molar concentration of the discharge source
$\frac{c_p}{c_v}$	Heat capacity ratio
D	Inner diameter of pipeline / vessel (m)
g_c	Gravitational constant (m^3/s^2kg)
K_f	Excess head loss
I	Static inventory in the continuous system (kg)
I_T	Thermal radiation ($kW/m^{2)}$
L	Length of the vessel / Level of the liquid (m)
M	Initial stored mass (kg)
P_1, P_2	1: Upstream, 2: Downstream gas pressure (Pa)
Q	Discharge mass flowrate (kg/s)
SI	Estimated static inventory (kg)
t	Time (s)
t_d	Release duration (s)
t_i	Time at time step i (s)

$t_{isolation}$	Isolation time (s)
t_{vf}	Duration of an air change with forced ventilation (s)
t_{vw}	Duration of an air change in building with multiple vents during gas leak (s)
t_w	Duration of an air change caused by wind (s)
V	Volume of the building indoors (m^3)
v	Volumetric flowrate (m^3/s)
v_f	Volumetric flowrate at forced ventilation (m^3/s)
v_{in}	Total volumetric flowrate of gas flows from outside to inside (m^3/s)
v_o	Volumetric flowrate of continuous discharge (m^3/s)
$v_{o,i}$	Volumetric flowrate of discharge at time step i (m^3/s)
v_{out}	Total volumetric flowrate of gas flows from inside to outside (m^3/s)
v_w	Volumetric flowrate caused by wind in indoors (m^3/s)
Y	Gas expansion factor
ρ_f	Fluid density (kg/m^3)
ρ_1	Upstream fluid density (kg/m^3)

References

[1] Baybutt, P. Insights into process safety incidents from an analysis of CSB investigations, *Journal of Loss Prevention in the process industries*, 2016, 43, 537-548

[2] Gould J.; Glossop, M.; Ioannides A. Review of hazard identification techniques, *Health and Safety Laboratory*, 2000.

[3] Khan, F.; Rathnayaka, S.; and Ahmed, S. Methods and models in process safety and risk management: Past, present, and future, *Process Safety and Environmental Protection*, 2016, *98*, 116-147.

[4] Khan, F.; Abbasi, S. A. Major accidents in process industries and an analysis of causes and consequences, *Journal of Loss Prevention in the Process Industries*, 1999, *12*, 361-378.

[5] Van Den Bosh C. J. H.; Weterings, R. A. P. M. Methods for the Calculation of Physical Effects (Yellow Book), Committee for the Prevention of Disasters, The Hague, Netherlands. 1997.

[6] CCPS. Guidelines for Evaluating the Characteristics of Vapor Cloud Explosions, Flash Fires, and BLEVEs, *American Institute of Chemical Engineers*, New York, NY. 1994.

[7] Bubbico R.; Mazzarotta, B. Accidental release of toxic chemicals: Influence of the main input parameters on consequence calculation, *Journal of Hazardous Materials*, 2004, *151*, 394-406.

[8] CCPS. Guidelines for Chemical Process Quantitative Risk Analysis, *American Institute of Chemical Engineers*, 1989.

[9] Crane Co. Flow of fluids through valves, fittings, and pipe, Technical paper No. 410. 1986.

[10] Woodward, J. L. A Model of Indoor Releases with Recirculating Ventilation, *Process Safety Progress*, 2000. *19*, *3*, 160-165.

[11] Wu, Y.; Yu, E.; Xu, Y. Simulation and analysis of indoor gas leakage, *Proceedings: Building Simulation*, *2007*, 1267-1271.

[12] Montoya, M.; Planas. E.; Casal J. A comparative analysis of mathematical models for relating indoor and outdoor toxic gas concentrations in accidental releases, *Journal of Loss Prevention in the Process Industries*, 2009, *22*, 381-391.

[13] Deaves, D.; Gilham, S.; Spencer, H. Mitigation of dense gas releases in buildings: use of simple models, *Journal of Hazardous Materials*, 2000, *71*, 129-157.

[14] Gilham, S.; Deaves, D. M.; Woodburn, P. Mitigation of dense gas releases within buildings: validation of CFD modeling, *Journal of Hazardous Materials*, 2000, *71*, 193-218.

[15] Dong, L.; Zuo, H.; Hu, L.; Yang, B.; Li L.; Wu, L. Simulation of heavy gas dispersion in a large indoor space using CFD model, *Journal of Loss Prevention in the Process Industries*, 2017, *46*, 1-12.

[16] Jiao, Z.; Yuan, S.; Ji, C.; Mannan, M. S.; Wang, Q. Optimization of dilution ventilation layout design in confined environments using Computational Fluid Dynamics (CFD), *Journal of Loss Prevention in the Process Industries*, 2019, *60*, 195-202.

[17] Awbi, H. B. Energy efficient ventilation for retrofit buildings. *In: Proceedings of 48th AiCARR international conference on energy performance of existing buildings*, 2011, 23-46.

[18] Cao, G.; Awbi, H.; Yao, R.; Fan, Y.; Sirén, K.; Kosonen, R.; Zhang, J. A review of the performance of different ventilation and airflow distribution systems in buildings, *Building and Environment*, 2014, *73*, 171-186.

[19] Baldwin, P. E. J.; Maynard, A. D. A survey of wind speeds in indoor workplaces, *The Annals of occupational hygiene*, 1998, *42(5)*, 303-313.

[20] Gilham, S.; Deaves, D. M.; Hoxey, R. P.; Boon, C. R.; Mercer, A. Gas build-up within a single building volume – comparison of measurements with both CFD and simple zone modelling, *Journal of Hazardous Materials*, 1997, *53*, 93-114.

[21] Gavelli, F.; Davis, S. G.; Hansen, O. R. Evaluating the potential for overpressures from the ignition of an LNG vapor cloud during offloading, *Journal of Loss Prevention in the Process Industries*, 2011, *24*, 908-915.

[22] Wilson, D. J.; Kiel, D. E. Gravity driven counterflow through an open door in a sealed room, *Building and Environment*, 1990, *25(4)*, 379-388.

[23] Lim, H.; Um, K.; Jung, S. A study on effective mitigation system for accidental toxic gas releases, *Journal of Loss Prevention in the Process Industries*, 2017, *49(B)*, 636-644.

[24] Mannan, S. Lees' Process Safety Essentials: Hazard Identification, *Assessment and Control*. Butterworth-Heinemann, 2013

[25] Khan, F. I.; Amyotte, P. R. Inherent safety in offshore oil and gas activities: a review of the present status and future directions. *Journal of Loss Prevention in the Process Industries*. 2002, *15*(4), 279-289.

[26] Bernechea, E. J.; Arnaldos, J. Optimizing the design of storage facilities through the application of ISD and QRA. *Process Safety and Environmental Protection*. 2014, *92*(6), 598-615.

[27] Khan, F. I.; Amyotte, P. R. I2SI: a comprehensive quantitative tool for inherent safety and cost evaluation, *Journal of Loss Prevention in the Process Industries*, 2005, *18*, 310–326.

[28] Shah, N. M; Hoadley, A. F; Rangaiah, G. P. Inherent safety analysis of a propane precooled gas-phase liquefied natural gas process. *Industrial & Engineering Chemistry Research*. 2009, *48*(10), 4917-4927.

[29] Eini, S.; Abdolhamidzadeh, B.; Reniers, G.; Rashtchian, D. Optimization procedure to select an inherently safer design scheme. *Process Safety and Environmental Protection*. 2015, *93*, 89-98.

[30] Eini, S.; Shahhosseini, H. R.; Javidi, M.; Sharifzadeh, M.; Rashtchian, D. Inherently safe and economically optimal design using multi-objective optimization: the case of a refrigeration cycle. *Process Safety and Environmental Protection.* 2016, *104,* 254-267.

[31] Jafari, M. J.; Mohammadi, H.; Reniers, G.; Pouyakian, M.; Nourai, F.; Torabi, S. A.; Miandashti, M. R. Exploring inherent process safety indicators and approaches for their estimation: A systematic review. *Journal of Loss Prevention in the Process Industries*. 2018, *52*, 66-80.

[32] Lawrence, D. Quantifying inherent safety of chemical process routes. *Doctoral dissertation, © Duncan Lawrence*, 1996.

[33] Heikkilä, A. M. Inherent safety in process plant design: an index-based approach. VTT Technical Research Centre of Finland, 1999.

[34] Palaniappan, C.; Srinivasan, R.; Tan, R. Selection of inherently safer process routes: a case study. *Chemical Engineering and Processing: Process Intensification*. 2004, *43*(5), 641-647.

[35] Edwards, D. W.; Lawrence, D. Assessing the inherent safety of chemical process routes: is there a relation between plant costs and inherent safety? *Chemical Engineering Research and Design*, 1993, *71(B)*, 252-258.

[36] Heikkilä, A. M.; Markku, H.; Järveläinen, M. Safety Considerations in process synthesis, *Computers and Chemical Engineering*, 1996, *20*, S115-S120.

[37] Rangaiah, G. P.; Bonilla-Petriciolet, A. *Multi-objective optimization in chemical engineering: developments and applications*. John Wiley & Sons, 2013.

[38] Athar, M.; Shariff, A. M.; Buang, A.; Zaini, D. Integrated safety and process optimization approach for ammonia synthesis loop. *International Journal of Automotive and Mechanical Engineering.* 2018, *15(1)*, 5074-5085.

[39] Shariff, A. M.; Rusli, R.; Leong, C. T.; Radhakrishnan, V. R.; Buang, A. Inherent safety tool for explosion consequences study. *Journal of Loss Prevention in the Process Industries*. 2006, *19*(5), 409-418.

[40] Shariff, A. M.; Zaini, D. Toxic release consequence analysis tool (TORCAT) for inherently safer design plant. *Journal of hazardous materials*. 2010, *182*(1-3), 394-402.

[41] Shariff, A. M.; Wahab, N. A.; Rusli, R. Assessing the hazards from a BLEVE and minimizing its impacts using the inherent safety concept. *Journal of Loss Prevention in the Process Industries*. 2016, *41*, 303-314.

[42] Ruiz-Femenia, R.; Fernández-Torres, M. J.; Salcedo-Díaz, R.; Gómez-Rico, M. F.; Caballero, J. A. Systematic tools for the conceptual design of inherently safer chemical processes. *Industrial & Engineering Chemistry Research*. 2017, *56*(25), 7301-7313.

[43] Vázquez, D.; Ruiz-Femenia, R.; Jiménez, L.; Caballero, J. A. Multiobjective Early Design of Complex Distillation Sequences Considering Economic and Inherent Safety Criteria. *Industrial & Engineering Chemistry Research*. 2018, *57*(20), 6992-7007.

[44] Leong, C. T.; Shariff, A. M. Process route index (PRI) to assess level of explosiveness for inherent safety quantification. *Journal of Loss Prevention in the Process Industries*. 2009, *22*(2), 216-221.

[45] Lee, Y.; Huh, C.; Lee, W.; Inherently safer process design of natural gas liquefaction processes through multiobjective optimization-part 1. with inherent safety indexes. *Industrial & Engineering Chemistry Research.* 2019, *58*(10), 4186-4198.

[46] Venkatarathnam, G.; Timmerhaus, K. D. Cryogenic Mixed Refrigerant Processes (Vol. 100). New York: Springer, 2008.

[47] Ronza, A.; Vílchez, J. A.; Casal, J. Using transportation accident databases to investigate ignition and explosion probabilities of flammable spills. *Journal of Hazardous Materials*. 2007, *146*, 106-123.

[48] HSE, Failure rate and event data use within risk assessments. *The Health and Safety Executive*. 2012.

[49] International Association of Oil & Gas Producers. Risk Assessment Data Directory. Report No. 434. 2010.

[50] CCPS, Guidelines for Consequence Analysis of Chemical Releases. *AIChE*, 1999.

[51] Mercx, W. P. M.; van den Berg, A. C. Methods for the Calculation of Physical Effects (The Yellow Book). *TNO*, 1997.

[52] Finney, D. J. Probit Analysis, *Cambridge University Press*, 1971.

[53] Methods of approximation and determination of human vulnerability for offshore major accident hazard assessment, *HSE*, 2006

[54] CCPS, Guidelines for Vapor Cloud Explosion, Pressure Vessel Burst, BLEVE, and Flash Fire Hazards, 2nd Ed. *AIChE*, 2010.

[55] Grodzevich, O.; Romanko, O. Normalization and other topics in multi-objective optimization, 2006.

[56] Hwang, C. L.; Lai, Y. J.; Liu, T. Y.; A new approach for multiple objective decision making. *Computers and Operational Research*. 1993. *20(8)*. 889-899.

[57] Nădăban, S.; Dzitac, S.; Dzitac, I. Fuzzy TOPSIS: a general view. *Procedia Computer Science*, 2016, *91*, 823-831.

[58] Shariff, A. M.; Leong, C. T.; Zaini, D. Using process stream index (PSI) to assess inherent safety level during preliminary design stage. *Safety science*. 2012, *50*(4), 1098-1103.

Abstract in Korean (국문초록)

화학 공정 안전은 공정의 위험을 평가하기 위해 수행된다. 여러 기법들 중 일반적으로 공정 관리 단계에서는 다양한 기법이 사용되지만, 특히 공정 안전성과 위험성을 정확하게 평가하고 분석하려면 서로 다른 설계나 대안 등과 직접적인 비교를 가능하게 하는 정량적 방법이 필요하게 된다. 하지만 특성과 복잡성이 다른 다양한 공정들이 존재하기 때문에 각 공정의 특성에 따라 안전을 고려해야 하고, 초기 설계 단계부터 운영 단계까지 안전을 고려한 화학 공정 설계 방법을 확립하는 것이 중요하다. 그러나 QRA (Quantitative Risk Assessment) 또는 HAZOP (Hazard and Operability study) 연구와 같은 대부분의 공정 안전 접근 방식은 설계 절차 마지막에 고려되고, 종종 반복적이거나 시간 소모적인 특성으로 인해 긴 시간과 많은 비용이 드는 단점이 존재한다. 따라서 본 연구는 공정의 경제적 타당성과 안전성을 동시에 고려하기 위해 본질적으로 안전한 공정을 설계하는 것을 목표로 하여 위험 기반 설계 방법과 설계에 필요한 모델링을 제안하였다. 따라서 본 논문에서는 공정 설계 및 운영 중에 발생할 수 있는 위험을 분석하고 이해하는 데 필요한 시스템 구성을 위해 공정 지식 관리, 공정 안전 정보, 내재적으로 안전한 설계, 공정 위험 분석, 프로젝트 경제성 검토 등의 요소들을 다루었다. 이를 적용할 공정으로는 최근 셰일 가스 및 중소규모 가스전 등의 개발로 주목 받고 있는 천연가스 관련 공정을 선정하여 최종적으로 다목적 최적화를 통한 LNG 액화 공정의 최적 설계를 결정하는 것을 목표로 하였다. 본

논문의 2장에서는 화학사고 결과 모델링에 대해 다루어 화학 공정에서 사용되는 모델들에 대한 분석이 행해졌으며 추가로 필요하다고 고려되는 실내 유출 모델에 대한 개발 및 검증이 제시되었다. 3장에서는 공정 정보를 사고 모델링에 사용하는 인터랙티브 시뮬레이션에 대해서 다루었다. 최종적으로 4장에서 이상의 결과물들을 적용하여 보다 안전한 공정을 설계하기 위한 목적으로 내재적 안전성의 개념을 도입한 다목적 최적화 방법론을 제시하였으며, 이를 천연가스 액화공정의 예비 설계단계에 적용하여 경제성과 안전성을 동시에 고려한 결과를 찾아냈다. 이 과정에서 기존 내재적 안전성을 고려한 설계들이 가지고 있던 한계를 정량적 위험성 평가 절차를 최적화 과정에 직접 구현하는 것을 통해 보완하였다.

키워드: 위험성 기반 설계, 내재적 안전성, 위험성 추정, 정량적 위험성 평가

학번: 2014-21537